FR-PHENO-2015-008

arXiv:1511.01698v1 [hep-ph] 5 Nov 2015

Non-factorizable photonic corrections to resonant production and decay of many unstable particles

Stefan Dittmaier and Christopher Schwan

Albert-Ludwigs-Universität Freiburg, Physikalisches Institut,
D-79104 Freiburg, Germany

Abstract:

Electroweak radiative corrections to the production of high-multiplicity final states with several intermediate resonances in most cases can be sufficiently well described by the leading contribution of an expansion about the resonance poles. In this approach, also known as pole approximation, corrections are classified into separately gauge-invariant factorizable and non-factorizable corrections, where the former can be attributed to the production and decay of the unstable particles on their mass shell. The remaining non-factorizable corrections are induced by the exchange of soft photons between different production and decay subprocesses. We give explicit analytical results for the non-factorizable photonic virtual corrections to the production of an arbitrary number of unstable particles at the one-loop level and, thus, deliver an essential building block in the calculation of next-to-leading-order electroweak corrections in pole approximation. The remaining virtual factorizable corrections can be obtained with modern automated one-loop matrix-element generators, while the evaluation of the corresponding real photonic corrections can be evaluated with full matrix elements by multi-purpose Monte Carlo generators. Our results can be easily modified to non-factorizable QCD corrections, which are induced by soft-gluon exchange.

November 2015

1 Introduction

With very few exceptions, all interesting fundamental particles are unstable and can only be reconstructed after collecting their decay products in detectors. In the Standard Model (SM), this most notably concerns the gauge bosons W and Z of the weak interaction, the top quark, and the Higgs boson, for which a candidate was found at the LHC in 2012. In extensions of the SM, typically more heavy, unstable particles are predicted, such as additional Higgs bosons or gluinos, charginos, neutralinos, and sfermions in supersymmetric theories. After the first period of data taking at the LHC, the SM is in better shape than ever in describing practically all phenomena in high-energy particle physics. The search for new physics, thus, has to proceed with precision at the highest possible level, in order to reveal any possible deviation from SM predictions. To this end, both QCD and electroweak corrections have to be included in cross-section predictions.

Production processes of unstable particles notoriously lead to many-particle final states where the bulk of cross-section contributions results from phase-space regions where the intermediate unstable particles are resonant, i.e. near their mass shell. In the usual perturbative evaluation of scattering amplitudes in quantum field theory, a particle propagator develops a pole at the resonance point, i.e. a proper resonance description requires at least a partial resummation of self-energy corrections to the propagator near the resonance. Since this procedure mixes perturbative orders, such Dyson summations potentially lead to violations of identities (Ward, Slavnov–Taylor, Nielsen identities) that manifest gauge invariance order by order in perturbation theory. A more detailed discussion of this issue and further references can be found in Ref. [1]. The two most prominent procedures to avoid the gauge breaking are the so-called *pole scheme* [2, 3] and the *complex-mass scheme* [4, 5]. Both make use of the fact that the complex pole location $p^2 = \overline{M}^2$ of an unstable particle's propagator with momentum transfer p is a gauge-invariant quantity which can serve for a proper mass and decay width definition [6, 7]. In the complex-mass scheme the complex masses are consistently introduced as input parameters, so that all coupling parameters derived from the masses, like the electroweak mixing angle in the SM, become complex. Being a consistent analytical continuation to complex parameters, this scheme fully maintains gauge invariance.[1] The scheme delivers the same level of accuracy in resonant and non-resonant regions in phase space. However, if one is only interested in the resonance regions, which is typically the case in many-particle processes with low cross sections, the scheme leads to a proliferation of terms induced by the numerous Feynman diagrams contributing only in off-shell regions.

The pole scheme suggests to isolate the gauge-invariant residues of the resonance poles and to introduce propagators with complex masses $\overline{M}$ only there, while keeping the remaining parts untouched. Restricting this general procedure to resonant contributions defines the *pole approximation* (PA), which is adequate if only the off-shell behaviour of cross sections near resonances is relevant, but contributions deep in the off-shell region are negligible. The corrections to the resonance residues comprise the corrections to the pro-

[1] The complex-mass scheme introduces spurious unitarity violation, which is, however, always beyond the level of completely calculated orders [8], i.e. the spurious terms are of next-to-next-to-leading order in next-to-leading order calculations, etc.

duction and decay subprocesses with on-shell kinematics for the resonant particles. Since these contributions to matrix elements contain explicit resonance factors $\propto 1/(p^2 - \overline{M}^2)$, they are called *factorizable* corrections. The remaining resonant contribution in the PA furnish the *non-factorizable* corrections. They result from the fact that the infrared (IR) limit in loop diagrams and in real emission contributions and the procedure of setting particle momenta on their mass shell do not commute with each other if the on-shell limit leads to soft IR singularities. This is the case if a soft (real or virtual) massless gauge boson bridges a resonance. The fact that only the soft momentum region of the massless gauge boson leads to resonant contribution simplifies the calculation of the non-factorizable corrections, because factorization properties of the underlying diagrams can be exploited. The terminology "non-factorizable", thus, does not refer to factorization properties of diagrammatic parts, but to the off-shell behaviour of the corrections, which apart from resonance factors $1/(p^2 - \overline{M}^2)$ contain non-analytic terms like $\ln(p^2 - \overline{M}^2)$.

The complex-mass and pole schemes were successfully used in many higher-order calculations, both for electroweak and QCD corrections. Here we just mention the two examples of single and pair production of the weak gauge bosons W and Z, where results of the two schemes have been compared in detail. For W-pair production at LEP2, $e^+e^- \to WW \to 4\,\text{fermions}$, the *double-pole approximation* (DPA) for the two W resonances was worked out in different next-to-leading-order (NLO) variants [9, 10, 11, 12], which were numerically compared in detail [13]. Later the comparison to the full off-shell NLO calculation [5, 14] within the complex-mass scheme confirmed both the expected accuracy of the DPA in the resonance region and the limitation in the transition region to the off-shell domains. The situation is expected to be similar for W-pair production at hadron colliders, where up to now only results in DPA are known [15, 16]. For the conceptionally simpler Drell–Yan process of single W/Z production at hadron colliders, detailed comparisons between PA and complex-mass scheme are discussed in Refs. [17, 18]. In Ref. [18] the concept of a PA was carried to the next-to-next-to-leading-order level and applied to the mixed QCD–electroweak corrections of $\mathcal{O}(\alpha_s\alpha)$. Applications of the PA to processes with more than two resonances only exist for leading-order (LO) predictions (see, e.g., Ref. [19]).

The concept of the PA can be carried out both for virtual and real radiative corrections, however, care has to be taken that the approximations are set up in such a way that the cancellation of IR (soft and/or collinear) singularities between virtual and real corrections is not disturbed. If both virtual and real corrections are treated in PA, the sum of virtual and real non-factorizable corrections forms a closed gauge-invariant, IR-finite subset of corrections that can be discussed separately. For single and double resonances it has been shown that these completely cancel at NLO [20, 21] (i.e. up to the level of non-resonant contributions) if the virtuality of the resonances is integrated over, as done in integrated cross sections or most of the commonly used differential distributions. For invariant-mass distributions of resonating particles, non-factorizable corrections are non-vanishing, but turn out to be numerically small as, e.g., discussed in the literature for single W/Z production [18], even to $\mathcal{O}(\alpha_s\alpha)$, or for the production of W-boson pairs [22, 23, 24] or Z-boson pairs [25].

The smallness of the sum of virtual and real non-factorizable corrections poses the question about their relevance. Apart from the fact that there is no guarantee that those

effects are negligible unless they are calculated, the virtual non-factorizable corrections alone represent an important building block in the ongoing effort of the high-energy community in automating NLO QCD and electroweak corrections to multi-particle processes. On the side of real NLO corrections, the required evaluation of full LO amplitudes, together with an appropriate subtraction of IR singularities, is under control for up to 8−10 final-state particles by automated systems such as SHERPA [26, 27], MADGRAPH [28, 29], or HELAC-NLO [30, 31]. On the other hand, the much more complex evaluation of virtual one-loop amplitudes is confined to lower multiplicities in spite of the great progress in recent years reached by the one-loop matrix-element generators such as BLACKHAT [32], GOSAM [33], HELAC-NLO [30], MADLOOP [34], NJET [35], OPENLOOPS [36] and RECOLA [37]. A promising approach to drive automation to higher multiplicities in production processes with several unstable particles in resonances—in particular in view of electroweak corrections—is, thus, to make use of full matrix elements in LO and on the side of the real corrections, but to employ the PA for the virtual parts. The factorizable virtual corrections can then be obtained with the above one-loop matrix-element generators, accompanied by the non-factorizable virtual corrections, for which we give explicit analytical results in this paper. We note in passing that this kind of hybrid approach was already used in the Monte Carlo generator RACOONWW [4, 11, 12, 38] for W-pair production in e^+e^- annihilation.

In detail, we present generic results on the non-factorizable virtual corrections for the production of arbitrarily many resonances and their decays, i.e. we do not consider resonances that are part of cascade decays. Moreover, we restrict our calculation to electroweak corrections to keep the derivation and results transparent, but the modifications needed for QCD corrections are straightforward. Similar results were given in Ref. [15], but without detailed derivation and somewhat less general. Technically, pole expansions can be carried out on the basis of scattering amplitudes, as done, e.g., in Refs. [21, 22, 23, 24, 17, 15, 18], or alternatively with the help of specifically designed effective field theories, as formulated in Refs. [39, 40]. In this paper, we entirely analyze scattering amplitudes using the Feynman-diagrammatic approach.

The paper is organized as follows: In Sec. 2 we set our conventions and notations and review the general structure of the pole approximation, including the definition of factorizable and non-factorizable corrections. Moreover, our strategy for calculating the non-factorizable corrections is explained in detail there. Section 3 contains both our general results and their illustration in applications to the Drell–Yan process, to vector-boson pair production, and to vector-boson scattering. Our conclusions are presented in Sec. 4. The appendices provide more details about the derivation of our central results as well as supplementary formulas that are helpful in the implementation of our results in computer codes.

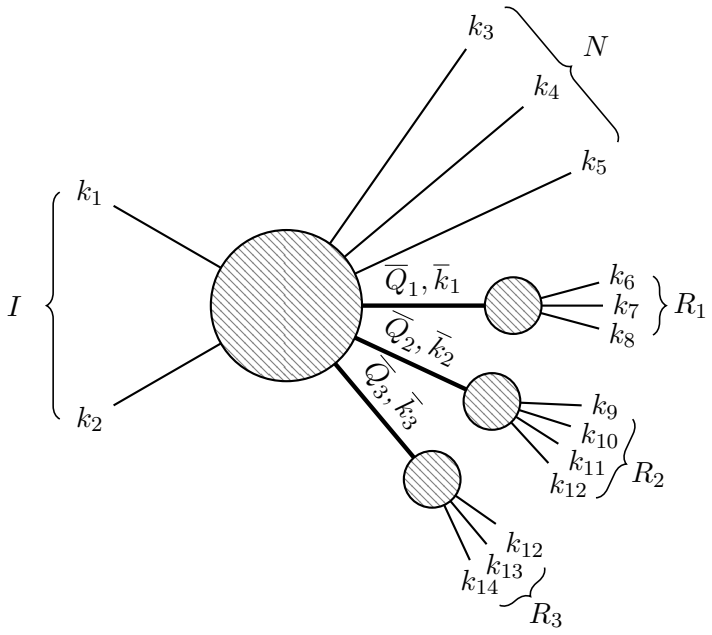

Figure 1: Diagram for a typical process with multiple resonances illustrating the labelling of external particles for a process $I \to F = N \cup R$. The particles with indices $i \in I$ are incoming, particles with indices $i \in F$ are outgoing. The outgoing particles either result from the decay of a resonant particle, $i \in R$, or are directly produced without intermediate resonant state, $i \in N$. There are r resonances which have electric charges $\overline{Q}_j$ and momenta $\overline{k}_j$ with $j \in \overline{R} = \{1, \ldots, r\}$. The decay products of resonance j are labelled with $i \in R_j$.

2 Pole approximation and non-factorizable corrections

2.1 Conventions and notations

Our conventions for labelling particles and momenta are illustrated in Fig. 1. We distinguish between initial- and final-state particles where a final-state particle is either one of the n non-resonant particles or a decay product of one of the r resonant intermediate states.

We define the index set I comprising the indices of incoming particles, the r sets R_j containing the indices of the decay products of resonance j, the set $\overline{R}$ of all r resonances, and finally the set N collecting the n remaining particles. Typically we have $I = \{1, 2\}$ and therefore $|I| = 2$, although we are not limited to this case. In summary, the numbers for resonant and non-resonant particles are related to the index sets by

$$|R_j| = r_j, \quad j \in \overline{R} \equiv \{1, \ldots, r\}, \tag{2.1a}$$

$$|N| = n. \tag{2.1b}$$

For convenience we define

$$F = N \cup R, \quad R = \bigcup_{j=1}^{r} R_j, \tag{2.2}$$

i.e. F is the index set of all outgoing particles. The momentum of external particle i is labelled with k_i for $i \in I \cup F$, where momenta are defined to be outgoing. Incoming particles with incoming momenta $p_i, i \in I$, therefore have momentum $p_i = -k_i$. The resonant particle j has momentum

$$\overline{k}_j = \sum_{i \in R_j} k_i. \tag{2.3}$$

We define invariants in the following way,

$$s = \left(\sum_{i \in I} p_i\right)^2, \tag{2.4a}$$

$$s_{ij} = (k_i + k_j)^2, \qquad i,j \in I \cup F, \tag{2.4b}$$

$$\overline{s}_{ij} = (\overline{k}_i + k_j)^2 \qquad i \in \overline{R}, \quad j \in I \cup F, \tag{2.4c}$$

$$\tilde{s}_{ij} = (\overline{k}_i - k_j)^2, \qquad i \in \overline{R}, \quad j \in I \cup F, \tag{2.4d}$$

$$\overline{\overline{s}}_{ij} = (\overline{k}_i + \overline{k}_j)^2, \quad i,j \in \overline{R}, \tag{2.4e}$$

where whenever a quantity possesses a "bar" or a "tilde", it concerns a resonant (intermediate) particle. The asymmetric sign convention in the definition of $\overline{s}_{ij}$ and $\tilde{s}_{ij}$ accounts for the fact that the momenta of the resonances are outgoing/incoming in the production/decay subprocesses. The squared masses of the particles are

$$k_i^2 = m_i^2, \tag{2.5a}$$

$$\overline{M}_j^2 = M_j^2 - \mathrm{i} M_j \Gamma_j, \tag{2.5b}$$

where M_j and Γ_j are the real mass and width parameters of the unstable particle j. The final-state particles are taken to be massive, so that potential collinear singularities in the case of light particles are regularized by a small mass m_i. We also define the inverse propagator denominators with complex masses for the resonant particle j as

$$K_j = \overline{k}_j^2 - \overline{M}_j^2, \quad j \in \overline{R}. \tag{2.6}$$

In order to regularize soft IR divergences we use an infinitesimal photon mass $m_\gamma \to 0$ and give a simple substitution rule to translate our results to dimensional regularization in App. C.

Finally, each particle possesses an electric (relative) charge Q_i so that global charge conservation reads

$$\sum_{i \in I \cup F} Q_i \sigma_i = 0, \tag{2.7}$$

with sign factors σ_i that are positive, $\sigma_i = +1$, for incoming particles and outgoing antiparticles, and negative, $\sigma_i = -1$, for incoming antiparticles and outgoing particles. Local charge conservation for the resonance j and its decay products reads

$$\overline{Q}_j = -\sum_{i \in R_j} Q_i \sigma_i, \quad \sum_{j=1}^{r} \overline{Q}_j = \sum_{i \in I \cup N} \sigma_i Q_i, \tag{2.8}$$

where $\overline{Q}_j$ is the electric charge of the produced resonance j of particle or antiparticle type alike.

2.2 Structure of the pole approximation

2.2.1 Factorizable corrections

We define the LO matrix element in PA, $\mathcal{M}_{\mathrm{LO,PA}}$, as the product of the matrix elements for the production of r resonances with n additional non-resonant states N, $\mathcal{M}_{\mathrm{LO}}^{I\to N,R}$, and the matrix elements of the decays of each resonance j, $\mathcal{M}_{\mathrm{LO}}^{j\to R_j}$, multiplied by a product of r propagators of the resonant particles,

$$\mathcal{M}_{\mathrm{LO,PA}} = \sum_{\lambda_1,\dots,\lambda_r} \left(\prod_{i=1}^{r} \frac{1}{K_i}\right) \left[\mathcal{M}_{\mathrm{LO}}^{I\to N,R} \left(\prod_{j=1}^{r} \mathcal{M}_{\mathrm{LO}}^{j\to R_j}\right)\right]_{\left\{\overline{k}_l^2 \to \hat{\overline{k}}_l^2 = M_l^2\right\}_{l\in\overline{R}}} . \tag{2.9}$$

This product involves the sum over the polarizations λ_j of the resonances, inducing spin correlations between the different production and decay subprocesses. Note that the momenta of the resonances have to be set on shell in the matrix elements of the subprocesses, $\mathcal{M}_{\mathrm{LO}}^{I\to N,R}$ and $\mathcal{M}_{\mathrm{LO}}^{j\to R_j}$, otherwise the constructed matrix element is not gauge invariant in general. Since in PA we only keep the leading contribution in the expansion about the resonance poles, we can deform the original (off-shell) momenta $\overline{k}_i$ to momenta $\hat{\overline{k}}_i$ that are on the (real) mass shell, $\hat{\overline{k}}_l^2 = M_l^2$, which avoids the unpleasant appearance of complex momentum variables. The matrix element $\mathcal{M}_{\mathrm{LO,PA}}$ is, thus, the leading contribution of an expansion of the full matrix element of the process $I \to F$ in the limit $\Gamma_j \to 0$, where the widths Γ_j in the denominators $1/K_j$ are kept.

We emphasize that the LO matrix element in PA, $\mathcal{M}_{\mathrm{LO,PA}}$, is only an auxiliary quantity in NLO predictions in PA, while LO cross sections should be calculated with full LO matrix elements. Using $\mathcal{M}_{\mathrm{LO,PA}}$, e.g., in production processes of electroweak gauge bosons $V = \mathrm{W}, \mathrm{Z}$ would neglect already terms of relative order $\mathcal{O}(\Gamma_V/M_V) = \mathcal{O}(\alpha)$, which is of the generic order of NLO electroweak corrections.

The *factorizable corrections* by definition comprise all corrections to the various production and decay subprocesses, i.e. the corresponding matrix element $\mathcal{M}_{\mathrm{virt,fact}}$ is a sum of $r+1$ terms resulting from $\mathcal{M}_{\mathrm{LO,PA}}$ upon replacing one of the LO parts on the r.h.s. of Eq. (2.9) by the corresponding one-loop-corrected matrix element $\mathcal{M}_{\mathrm{virt}}$,

$$\begin{aligned}\mathcal{M}_{\mathrm{virt,fact,PA}} = \sum_{\lambda_1,\dots,\lambda_r} \left(\prod_{i=1}^{r} \frac{1}{K_i}\right) \Bigg[&\mathcal{M}_{\mathrm{virt}}^{I\to N,R} \prod_{j=1}^{r} \mathcal{M}_{\mathrm{LO}}^{j\to R_j} \\ &+ \mathcal{M}_{\mathrm{LO}}^{I\to N,R} \sum_{k=1}^{r} \mathcal{M}_{\mathrm{virt}}^{k\to R_k} \prod_{j\neq k}^{r} \mathcal{M}_{\mathrm{LO}}^{j\to R_j}\Bigg]_{\left\{\overline{k}_l^2 \to \hat{\overline{k}}_l^2 = M_l^2\right\}_{l\in\overline{R}}} .\end{aligned} \tag{2.10}$$

2.2.2 On-shell projection

Two different types of momenta enter Eqs. (2.9) and (2.10). The phase-space integral of the corresponding cross-section contribution usually is based on the full phase space determined by the momenta k_a of all final-state particles $a \in F$, where the intermediate momenta $\overline{k}_i$ are off their mass shell. These are the momenta entering the propagator

factor $\prod_i(1/K_i)$, while the partial matrix elements appearing in the square brackets are parametrized by *on-shell-projected momenta* $\hat{k}_a$ that result from all k_a by some deformation

$$\left\{k_i\right\}_{i\in I\cup F} \;\to\; \left\{\hat{k}_i\right\}_{i\in I\cup F} \tag{2.11}$$

in order to project the virtualities $\overline{k}_i^2$ of all resonances to their real mass shells at M_i^2, i.e.

$$\hat{\overline{k}}_i = \sum_{a\in R_i} \hat{k}_a, \qquad \hat{\overline{k}}_i^2 = M_i^2, \qquad i \in \overline{R}. \tag{2.12}$$

This on-shell projection has to respect overall momentum conservation and all mass-shell relations $k_a^2 = \hat{k}_a^2 = m_a^2$. Note that the projection involves some freedom, but the differences resulting from different definitions are of the order of the otherwise neglected non-resonant contributions.

We suggest the following on-shell projection (which is a generalization of the projection defined in Ref. [12]) for our considered class of processes with $r \geq 2$ resonances and possibly additional non-resonant particles in the final state. The on-shell projection preserves the momenta of the initial-state and non-resonant final-state particles, i.e.

$$\hat{k}_a = k_a \qquad a \in I \cup N. \tag{2.13}$$

We construct the on-shell-projected momenta by selecting pairs of i, j of resonances whose new momenta $\hat{k}_i$ and $\hat{k}_j$ are defined in their centre-of-mass frame, i.e. in the frame where $\overline{\boldsymbol{k}}_i + \overline{\boldsymbol{k}}_j = \sum_{a\in R_i\cup R_j} \boldsymbol{k}_a = 0$. In this frame the momenta of the two resonances are back-to-back and the velocities fixed by momentum conservation. We choose the direction of the on-shell-projected momentum $\hat{\overline{\boldsymbol{k}}}_i$ of resonance i along its original direction $\boldsymbol{e}_i = \overline{\boldsymbol{k}}_i/|\overline{\boldsymbol{k}}_i|$, which determines the on-shell-projected momenta as follows,

$$\hat{\overline{k}}_i^0 = \frac{\overline{\overline{s}}_{ij} + M_i^2 - M_j^2}{2\sqrt{\overline{\overline{s}}_{ij}}}, \qquad \hat{\overline{\boldsymbol{k}}}_i = \frac{\sqrt{\lambda(\overline{\overline{s}}_{ij}, M_i^2, M_j^2)}}{2\sqrt{\overline{\overline{s}}_{ij}}}\boldsymbol{e}_i, \tag{2.14a}$$

$$\hat{\overline{k}}_j^0 = \frac{\overline{\overline{s}}_{ij} - M_i^2 + M_j^2}{2\sqrt{\overline{\overline{s}}_{ij}}}, \qquad \hat{\overline{\boldsymbol{k}}}_j = -\hat{\overline{\boldsymbol{k}}}_i, \tag{2.14b}$$

where $\lambda(x, y, z) = x^2 + y^2 + z^2 - 2xy - 2xz - 2yz$ is the well-known triangle function. Note that this procedure leaves the sum of the two resonance four-momenta (and thus also their invariant mass $\overline{\overline{s}}_{ij}$) unchanged, $\hat{\overline{k}}_i + \hat{\overline{k}}_j = \overline{k}_i + \overline{k}_j$. Carrying out the procedure for all pairs of resonances in $\overline{R}$ completes the on-shell projection if their total number r is even. If there is an odd number of resonances, the remaining resonance is paired with an already projected resonance momentum (preferably one of Eq. (2.14b) where we did not preserve the direction) and repeat the procedure for this pair once again.

The on-shell projection of the decay products of each resonance can be done in a second step after fixing the resonance momenta $\hat{\overline{k}}_i$ as above. For simplicity we restrict ourselves to the case where a resonance i undergoes a $1 \to 2$ particle decay. Denoting the two decay

particles of i by a and b, i.e. $R_i = \{a, b\}$, we define the new momenta $\hat{k}_a$ and $\hat{k}_b$ in the centre-of-mass frame of $\hat{\overline{\boldsymbol{k}}}_i$ as

$$\hat{k}_a^0 = \frac{M_i^2 + m_a^2 - m_b^2}{2M_i}, \qquad \hat{\boldsymbol{k}}_a = \frac{\sqrt{\lambda(M_i^2, m_a^2, m_b^2)}}{2M_i}\boldsymbol{e}_a, \tag{2.15a}$$

$$\hat{k}_b^0 = \frac{M_i^2 - m_a^2 + m_b^2}{2M_i}, \qquad \hat{\boldsymbol{k}}_b = -\hat{\boldsymbol{k}}_a, \tag{2.15b}$$

where $\boldsymbol{e}_a = \overline{\boldsymbol{k}}_a/|\overline{\boldsymbol{k}}_a|$ is the direction of the original momentum $\overline{\boldsymbol{k}}_a$ in the centre-of-mass frame of $\hat{\overline{\boldsymbol{k}}}_i$. Note that this transformation is a simple rescaling of k_a and k_b if a and b are massless.

For processes with a single resonance it is not possible to leave all of the initial-state and non-resonant final-state momenta unmodified. In Sec. 3.2.1 we give a suitable on-shell projection for the case of no additional non-resonant particles and one resonance.

2.2.3 Non-factorizable corrections

Following the guideline of Ref. [24], we define the non-factorizable virtual correction as the difference between the full matrix element $\mathcal{M}_{\text{virt}}$ and the factorizable part in the PA, i.e.

$$\mathcal{M}_{\text{virt,nfact,PA}} \equiv \Big[\mathcal{M}_{\text{virt}} - \mathcal{M}_{\text{virt,fact,PA}}\Big]_{\text{res},\left\{\overline{k}_l^2, \overline{M}_l^2 \to M_l^2\right\}_{l\in\overline{R}}}, \tag{2.16}$$

where the subscript 'res' indicates that after performing the loop integration we keep only the resonant part of the expression. The additional subscript $\left\{\overline{k}_l^2, \overline{M}_l^2 \to M_l^2\right\}_{l\in\overline{R}}$ means that we set the virtualities and the complex masses of the resonances to their real mass shell whenever possible, i.e. when the replacements $\overline{k}_l^2 \to M_l^2$ and $\Gamma_l \to 0$ do not lead to singularities. Apart from the terms where $\overline{k}_l^2$ and $\overline{M}_l^2$ have to be kept, the non-factorizable matrix elements should be evaluated with on-shell projected momenta to produce a well-defined result.

The procedure for deriving $\mathcal{M}_{\text{virt,nfact,PA}}$ will be worked out in detail in Sec. 2.3 below. Here we just anticipate some basic features. In contrast to the factorizable parts the non-factorizable corrections receive contributions from diagrams in which the loop involves both production and decay of the resonances, so that the expression does no longer factor in the simple form of Eq. (2.10), justifying the name non-factorizable. However, as we will show in Sec. 2.3, the non-factorizable corrections can be written as

$$2\,\text{Re}\left\{\mathcal{M}_{\text{LO,PA}}^{*}\mathcal{M}_{\text{virt,nfact,PA}}\right\} \equiv |\mathcal{M}_{\text{LO,PA}}|^2\,\delta_{\text{nfact}}, \tag{2.17}$$

which defines the relative correction factor δ_{nfact}, for which we give an analytic expression in Sec. 3. In order to keep the derivation and the final results transparent, in this paper we restrict ourselves to the case of electroweak corrections, where only photon exchange turns out to be relevant.

2.3 Calculation of the non-factorizable corrections

2.3.1 Relevant Feynman diagrams

In Eq. (2.16) we have defined the non-factorizable corrections as the resonant parts of the difference between the full one-loop matrix elements and the factorizable terms. Thus, by definition the sum of the factorizable and non-factorizable corrections, defined in Eqs. (2.10) and (2.16), captures the full virtual correction in PA.

Although the definition of the non-factorizable corrections involves the full matrix element $\mathcal{M}_{\text{virt}}$, we do not need to know the full expression of $\mathcal{M}_{\text{virt}}$, since only a specific set of diagrams contributes to the non-factorizable parts. Following the arguments of Refs. [20, 21, 22, 23, 24], this set is identified as follows:

1. By definition, all diagrams that do not involve the resonance pattern of the considered process do not contribute to the resonant (factorizable or non-factorizable) corrections. Since resonance factors may also emerge from the loop integration, propagators in loops have to be included in the identification of potential resonances. In a first step, certainly all diagrams can be omitted that do not involve all relevant resonance propagators after omitting an internal line in the loop. After this step, we are left with two types of diagrams:

   (A) Diagrams in which at least one resonance propagator $j \in \overline{R}$ is confined in the loop. These are called *manifestly non-factorizable*.

   (B) Diagrams in which all resonance propagators appear at least on one tree-like line.

2. Among the diagrams of type (A) only those can develop a resonance corresponding to the propagator j that is confined in a loop if the loop contains a virtual photon exchanged between external particles and/or resonances of the process, because only then a soft IR divergence emerges.[2] This can be seen via simple power-counting in momentum space. Denoting the loop momentum on the propagator j by $\overline{k}_j + q$, the resonance factor $1/[(\overline{k}_j+q)^2-\overline{M}_j^2]$ receives support in the loop integration only within a phase-space volume in which each component of q is of $\mathcal{O}(|\overline{k}_j^2 - \overline{M}_j^2|/M_j) \sim \mathcal{O}(\Gamma_j)$. To compensate this suppression factor $\propto \Gamma_j^4$ in the four-dimensional loop integration, four powers of enhancement in the small momentum q are necessary. The only way to achieve this in a one-loop integral is a soft divergence by a photon exchange (or a gluon in the QCD case), a situation that can appear in two different ways. Firstly, the photon can be exchanged between two different external particles a and b, where the IR divergence is produced by the factor $1/[(q^2-m_\gamma^2)(q^2+2k_aq)(q^2-2k_bq)]$ composed of the three additional propagators. Secondly, the photon can be exchanged between an

[2] The exchange of a massless (or light) fermion does not produce the needed enhancement because of the additional momentum term $\not{q}$ in the propagator numerator. Massless or (light) scalars are ignored in this argument, since they are not part of the SM or of any favoured extension.

external particle a and another resonance $i \neq j$, where the IR divergence is produced by the factor[3] $1/[q^2 - m_\gamma^2)(q^2 + 2k_a q)(q^2 - 2\overline{k}_i q)]$.

3. The diagrams of type (B) already contribute to the factorizable corrections, because the respective loop subdiagrams contribute to an irreducible vertex function that can be attributed to the production or one of the decay subprocesses. Their factorizable contributions are obtained upon setting all momenta $\overline{k}_i$ ($i \in \overline{R}$) of the resonances to their mass shell everywhere but in the explicit propagator factors $1/K_i$. Since we are only interested in the leading contribution of the expansion about the resonances, we can neglect the decay widths Γ_i when setting $\overline{k}_i$ on shell, i.e. we can keep $\overline{k}_i^2 = M_i^2$ real, which conceptually and technically simplifies the evaluation of the factorizable corrections significantly. Diagrams of type (B) can, thus, only contribute to the non-factorizable corrections if the two steps of the loop integration and the transition to $\overline{k}_i^2 = M_i^2$ in the loop do not commute.[4] This can only happen if the process of setting $\overline{k}_i^2 \to M_i^2$ before the loop integration leads to a singularity for at least one resonance, which in turn is only the case if the loop contains a photon exchanged between resonance i and an external particle or another resonance.

In summary, non-factorizable corrections are due to diagrams that result from the corresponding LO diagrams by allowing for photon exchange between external particles of different subprocesses and resonances in all possible ways. The corresponding generic Feynman diagrams are illustrated in Fig. 2.

2.3.2 Extended soft-photon approximation

Considering the diagrams with non-factorizable contributions in more detail in momentum space, only loop momenta q of the internal photon with components of $\mathcal{O}(\Gamma_i)$ can contribute to the non-factorizable corrections, where Γ_i generically stands for the energy scale determined by the decay widths of the resonances. For diagrams of type (A) this is obvious, for diagrams of type (B) this is a consequence of the fact that the difference between the full diagram and its factorizable part can only develop a resonant part for such small q. This observation is the basis for the evaluation of the non-factorizable contributions in "extended soft-photon approximation" (ESPA) which is a modification of the commonly used "soft-photon approximation", which is based on the eikonal currents of soft photons. The modification concerns the fact that the soft momentum q is kept in the denominators of the resonance propagators, but are neglected elsewhere as usual. In particular, q can be set to zero in the numerator of Feynman diagrams and in the

[3]The factor $1/(q^2 - 2\overline{k}_i q)$ actually results from a decomposition of photon radiation off i into parts corresponding to production and decay of resonance i, which is achieved via a partial fractioning of propagators as shown in Eqs. (2.22a) and (2.22b) below. Without this decomposition this factor reads $1/[(\overline{k}_i - q)^2 - \overline{M}_i^2]$, i.e. the enhancement necessary in the power-counting argument exists for small $q \sim \mathcal{O}(\Gamma_i)$.

[4]In the full contribution the loop integration is done first, followed by the identification of the resonant parts upon taking $\overline{k}_i^2 \to M_i^2$. In the factorizable contributions $\overline{k}_i^2 = M_i^2$ is set in the integrand before the loop integration.

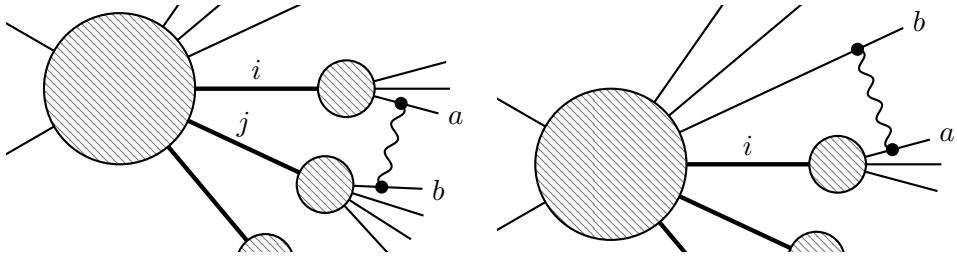

(a) ff′

(b) nf

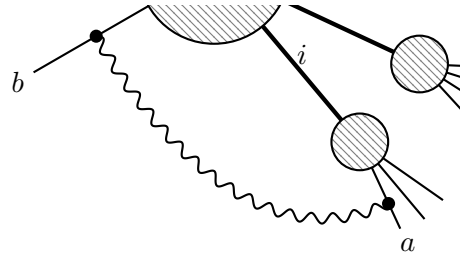

(c) if

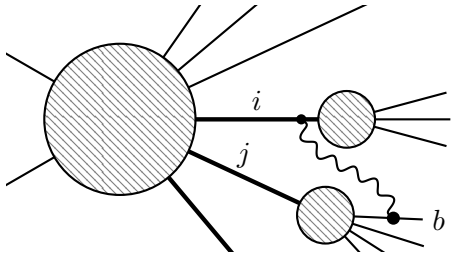

(d) mf′

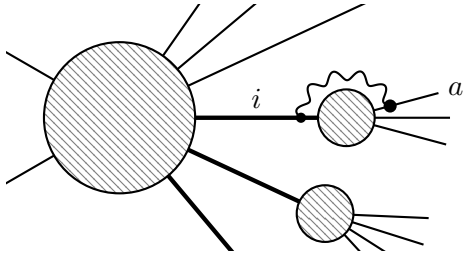

(e) mf

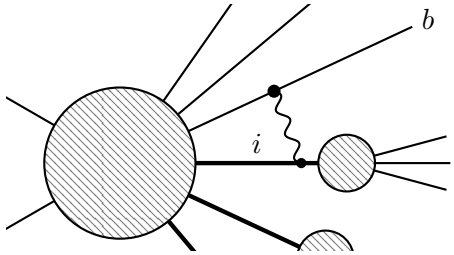

(f) mn

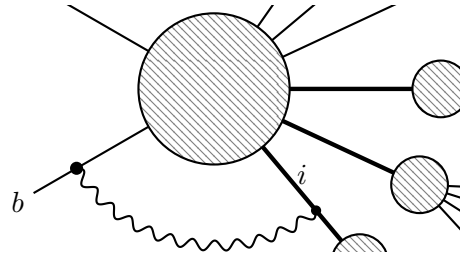

(g) im

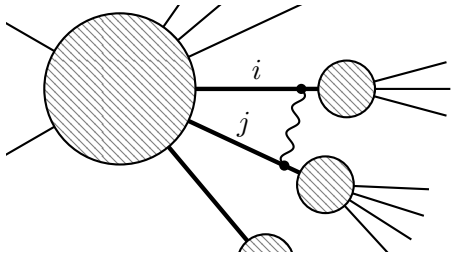

(h) mm′

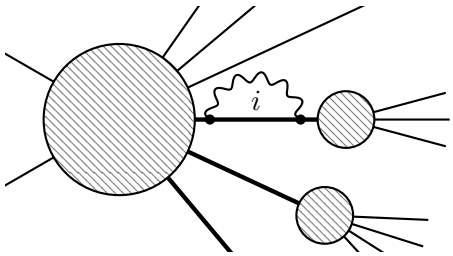

(i) mm

Figure 2: Feynman diagrams that contribute to the non-factorizable photonic corrections. The diagrams 2a, 2b, 2c, and 2d are called *manifestly non-factorizable*, since they do not contain factorizable contributions. They are type (A) diagrams, as defined in Sec. 2.3.1. The remaining diagrams also have factorizable parts and thus are of type (B).

denominators of all propagators that do not contribute to the soft divergences mentioned above. As a consequence, the non-factorizable corrections can be deduced from scalar one-loop integrals (i.e. without integration momenta in the numerator) with at most five propagators in the loop integration (largest number of loop propagators in Fig. 2), and the resulting correction factorizes from the underlying LO diagram, as already anticipated in Eq. (2.17).

Now we are able to start with the generic construction of the non-factorizable contributions within the ESPA. The coupling of the soft photon to an external particle, either incoming or outgoing, within the ESPA is exactly the same as in the usual eikonal approximation, i.e. coupling the photon with outgoing momentum q to the external line a with momentum k_a and electric charge Q_a modifies the underlying LO amplitude by the eikonal current factor

$$j^\mu_{\mathrm{eik},a}(q) = -\frac{2e\sigma_a Q_a k_a^\mu}{q^2 + 2qk_a}, \tag{2.18}$$

where a can be incoming or outgoing with the sign $\sigma_a = \pm 1$ as defined before, but k_a is formally outgoing. Here and in the following, the q^2 term in a propagator denominator is always implicitly understood to contain Feynman's iϵ prescription according to $q^2 + \mathrm{i}\epsilon$. The usual soft-photon approximation combines the individual contributions to the eikonal currents to a full eikonal current $J^\mu_{\mathrm{eik}}(q) = \sum_a j^\mu_{\mathrm{eik},a}(q)$, where the sum runs over all external particles a, and the soft-photon factor that multiplies $|\mathcal{M}_{\mathrm{LO}}|^2$ is proportional to the integral $\int \mathrm{d}^D q\, J_{\mathrm{eik}}(q) \cdot J_{\mathrm{eik}}(-q)/(q^2 - m_\gamma^2)$. We will generalize the eikonal currents to ESPA currents upon including contributions from the resonances, so that individual currents can be attributed to the production and decay subprocesses, J_{prod} and $J_{\mathrm{dec},i}$. The factorizable corrections will then be identified with the diagonal contributions $J_{\mathrm{prod}}(q) \cdot J_{\mathrm{prod}}(-q)$ and $J_{\mathrm{dec},i}(q) \cdot J_{\mathrm{dec},i}(-q)$, while the non-factorizable corrections correspond to non-diagonal terms $J_{\mathrm{prod}}(q) \cdot J_{\mathrm{dec},i}(-q)$ and $J_{\mathrm{dec},i}(q) \cdot J_{\mathrm{dec},j}(-q)$, where the photon is exchanged by different subprocesses.

We first define the contributions of external particles to the ESPA currents. Taking into account that outgoing lines $a \in R_i$ always result from resonance $i \in \overline{R}$, we include the modification of the resonance factor by the photon momentum in the definition of the ESPA current factors,

$$j^\mu_a(q) = j^\mu_{\mathrm{eik},a}(q) \frac{K_i}{K_i(q)} = -\frac{2e\sigma_a Q_a k_a^\mu}{q^2 + 2qk_a} \frac{K_i}{K_i(q)}, \qquad a \in R_i,\ i \in \overline{R}, \tag{2.19a}$$

$$j^\mu_a(q) = j^\mu_{\mathrm{eik},a}(q) = -\frac{2e\sigma_a Q_a k_a^\mu}{q^2 + 2qk_a}, \qquad a \in I \cup N, \tag{2.19b}$$

where

$$K_i(q) = (\overline{k}_i + q)^2 - \overline{M}_i^2 = q^2 + 2q\overline{k}_i + K_i. \tag{2.20}$$

Photon radiation off a resonance $i \in \overline{R}$ can be described by similar factors, but their derivation is somewhat more involved. The first step in this derivation is to analyse the emission of a soft photon with momentum q off i, where the components of q are of $\mathcal{O}(\Gamma_i)$.

In App. A we show for the relevant cases of resonances with spin 0, 1/2, or 1 that

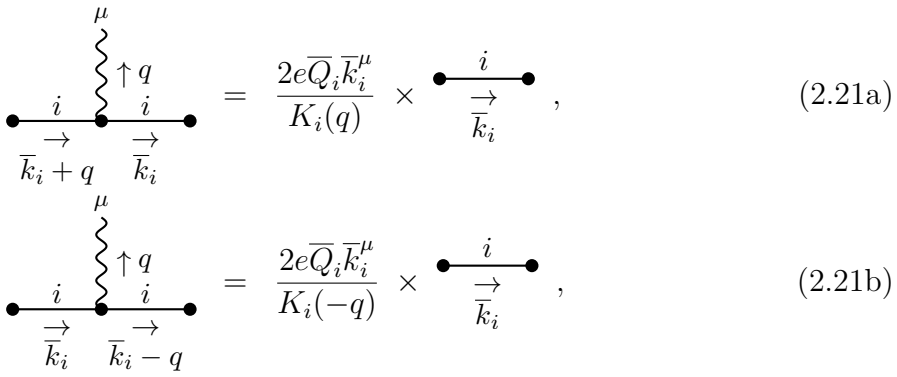

(2.21a)

(2.21b)

where the graphically represented propagators on the right-hand sides are proportional to $1/K_i$. Here, the charge $\overline{Q}_i$ refers to a particle or antiparticle flowing from the production part on the left to its decay part on the right. The subdiagram on the l.h.s. of Eq. (2.21a) belongs to a graph in which resonance i exchanges a photon with an external particle of the production part, or with another resonance $j \neq i$, or with any external particle of a final-state particle of any other resonance $j \neq i$. The second diagram belongs to the situation where the photon exchange happens between resonance i and one of its decay particles. In both situations the photon emission off the resonance can be split into an emission part before or after the resonant propagation using the partial fractionings

$$\frac{1}{K_i(q)K_i} = \frac{1}{q^2 + 2\overline{k}_i q}\left[\frac{1}{K_i} - \frac{1}{K_i(q)}\right], \tag{2.22a}$$

$$\frac{1}{K_i K_i(-q)} = \frac{1}{q^2 - 2\overline{k}_i q}\left[\frac{1}{K_i} - \frac{1}{K_i(-q)}\right]. \tag{2.22b}$$

Applied to the two subgraphs of Eqs. (2.21a) and (2.21b), this leads to

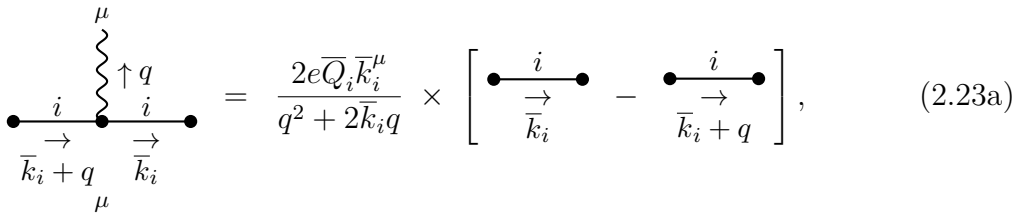

(2.23a)

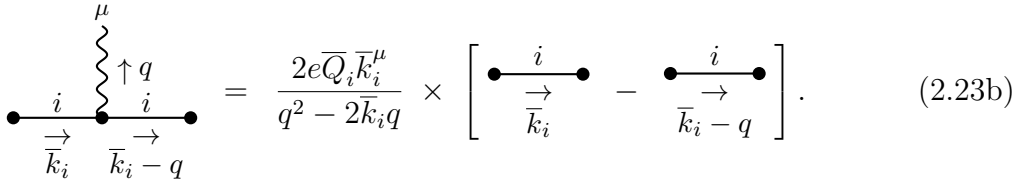

(2.23b)

The first contribution on the r.h.s. of Eq. (2.23a), which is proportional to $1/K_i$, corresponds to photon radiation during the production of the resonance. We attribute the ESPA current

$$\overline{j}^{\mu}_{\mathrm{out},i}(q) = \frac{2e\overline{Q}_i \overline{k}_i^{\mu}}{q^2 + 2\overline{k}_i q} \tag{2.24}$$

to an outgoing resonance i when it exchanges a photon with any particle of the production phase or the decay of any other resonance $j \neq i$. Applying this current factor to the corresponding LO matrix element describes soft-photon emission off a resonance of particle or antiparticle type during its production phase. The second subdiagram on the r.h.s. of Eq. (2.23a) corresponds to photon radiation during the decay of the resonance. We define the ESPA current

$$\overline{j}^{\mu}_{\mathrm{in},i}(q) = -\frac{2e\overline{Q}_i\overline{k}_i^{\mu}}{q^2 + 2\overline{k}_i q}\,\frac{K_i}{K_i(q)}, \tag{2.25}$$

which describes soft-photon emission off the resonance i during its decay phase. The factor $K_i/K_i(q)$ accounts for the fact that the propagator $1/K_i$ is included in the LO amplitude, but not $1/K_i(q)$. Using these results in combination with the ESPA currents (2.19a) describing radiation off the decay products, we can define the complete ESPA current $J^{\mu}_{\mathrm{dec},i}(q)$ for the decay of resonance i,

$$J^{\mu}_{\mathrm{dec},i}(q) = \overline{j}^{\mu}_{\mathrm{in},i}(q) + \sum_{a\in R_i} j^{\mu}_a(q) = \left[-\frac{2e\overline{Q}_i\overline{k}_i^{\mu}}{q^2 + 2\overline{k}_i q} - \sum_{a\in R_i}\frac{2e\sigma_a Q_a k_a^{\mu}}{q^2 + 2k_a q}\right]\frac{K_i}{K_i(q)}. \tag{2.26}$$

The combination $J_{\mathrm{dec},i}(q)\cdot J_{\mathrm{dec},j}(-q)$ is, thus, relevant for the non-factorizable corrections induced by photon exchange between the two decay subprocesses of two different resonances i and j.

The second type of photon emission, treated in Eq. (2.23b), is needed to describe photon exchange between a resonance i in its production phase and itself or one of its decay products. More precisely, it is the second term on the r.h.s. of Eq. (2.23b) that corresponds to this situation, since the corresponding i propagator carries the momentum $\overline{k}_i - q$, where the i momentum is reduced by photon radiation. For an outgoing resonance we define the ESPA current

$$\widetilde{j}^{\mu}_{\mathrm{out},i}(q) = -\frac{2e\overline{Q}_i\overline{k}_i^{\mu}}{q^2 - 2\overline{k}_i q}, \tag{2.27}$$

where we have not included the factor $K_i/K_i(-q)$ in the definition in order to avoid double counting this factor, because it is already included in the definition of $J^{\mu}_{\mathrm{dec},i}(-q)$ which will multiply $\widetilde{j}^{\mu}_{\mathrm{out},i}(q)$ in the calculation of the corresponding photon-exchange diagrams. The full ESPA current $J^{\mu}_{\mathrm{prod},i}(q)$ for the production of resonance i to describe photon exchange with the decay subprocess of i, then consists of three different types of contributions: the first where the photon is attached to resonance $i \in \overline{R}$, the second where the photon is attached to any other resonance $j \in \overline{R}, j \neq i$, and the third where the photon is attached to external stable particles $a \in I \cup N$, of the production phase,

$$\begin{aligned} J^{\mu}_{\mathrm{prod},i}(q) &= \widetilde{j}^{\mu}_{\mathrm{out},i}(q) + \sum_{\substack{j\in\overline{R}\\ j\neq i}} \overline{j}^{\mu}_{\mathrm{out},j}(q) + \sum_{a\in I\cup N} j^{\mu}_a(q) \\ &= -\frac{2e\overline{Q}_i\overline{k}_i^{\mu}}{q^2 - 2\overline{k}_i q} + \sum_{\substack{j\in\overline{R}\\ j\neq i}} \frac{2e\overline{Q}_j\overline{k}_j^{\mu}}{q^2 + 2\overline{k}_j q} - \sum_{a\in I\cup N}\frac{2e\sigma_a Q_a k_a^{\mu}}{q^2 + 2k_a q}. \end{aligned} \tag{2.28}$$

Since the first term in Eq. (2.23b) involves the propagator factor $1/K_i$ without photon momentum, this contribution corresponds to photon exchange between the resonance i during its decay phase and any particle taking part in the decay of i. This term in Eq. (2.23b) is, thus, only relevant for the factorizable soft-photonic corrections to the decay of i.

In summary, the complete set of non-factorizable contributions can be written as

$$\delta_{\mathrm{nfact}} = 2\,\mathrm{Re}\left\{(2\pi\mu)^{4-D}\int \mathrm{d}^D q\,\frac{-\mathrm{i}}{q^2-m_\gamma^2}\left[\sum_{i\in\overline{R}} J_{\mathrm{prod},i}(q)\cdot J_{\mathrm{dec},i}(-q)+\sum_{\substack{i,j\in\overline{R}\\ i\neq j}} J_{\mathrm{dec},i}(q)\cdot J_{\mathrm{dec},j}(-q)\right]\right\}, \tag{2.29}$$

in D dimensions in order to regularize occurring UV divergences. Setting m_γ to zero, directly produces the result for δ_{nfact} where soft IR divergences are regularized dimensionally. By construction, the correction factor δ_{nfact} is a gauge-invariant quantity. Its derivation starts from the difference (2.16) of the full matrix element and the corresponding factorizable corrections, which are both gauge invariant. Picking then the resonant parts from this difference in a consistent way and dividing it by $|\mathcal{M}_{\mathrm{LO,PA}}|^2$, leads to a gauge-invariant result. Electromagnetic gauge invariance is also reflected by the ESPA currents $J^\mu_{\mathrm{prod},i}(q)$ and $J^\mu_{\mathrm{dec},i}(q)$, since contracting them with q_μ gives zero up to terms of $\mathcal{O}(q^2)$, which, however, do only influence non-resonant contributions and are thus negligible. Therefore, in principle the ESPA currents and the non-factorizable corrections could be defined upon setting the q^2 terms to zero, as for instance done in Refs. [22, 23] for W-pair production. We have decided to keep the q^2 terms, firstly to be able to make direct use of standard scalar integrals, and secondly to avoid artificial ultraviolet divergences in non-resonant contributions.

It should be noted that r different ESPA currents $J^\mu_{\mathrm{prod},i}(q)$ are necessary to correctly describe photon exchange between the production of resonance i and the decay subprocesses of resonance j, since the momentum flows for $i=j$ and $i\neq j$ are not the same.[5]

3 Analytic results for the non-factorizable corrections

3.1 Generic result

Having derived Eq. (2.29), it is straightforward to translate all individual contributions to the correction factor δ_{nfact} shown in Fig. 2 into a form expressed in terms standard scalar one-loop integrals. This task is carried out in detail in App. B, and some of the relevant one-loop integrals are collected in App. C. The explicit results are given by

$$\begin{aligned}\delta_{\mathrm{nfact}} = &-\sum_{i=1}^{r}\sum_{j=i+1}^{r}\sum_{a\in R_i}\sum_{b\in R_j}\sigma_a\sigma_b Q_a Q_b\frac{\alpha}{\pi}\,\mathrm{Re}\,\{\Delta\}\\ &-\sum_{i=1}^{r}\sum_{a\in R_i}\sum_{b\in N\cup I}\sigma_a\sigma_b Q_a Q_b\frac{\alpha}{\pi}\,\mathrm{Re}\,\{\Delta'\}\end{aligned} \tag{3.1}$$

[5] This fact was already realized in the calculation of non-factorizable corrections to $e^+e^-\to \mathrm{WW}\to 4f$ in Refs. [22, 23], but overlooked in the (correct) calculation of Ref. [24] where currents were only introduced for illustration.

with functions

$$\Delta(i,a;j,b) = \Delta_{\mathrm{mm}} + \Delta_{\mathrm{mf}} + \Delta_{\mathrm{mm}'} + \Delta_{\mathrm{mf}'} + \Delta_{\mathrm{ff}'}, \tag{3.2a}$$

$$\Delta'(i,a;b) = \Delta'_{\mathrm{mm}} + \Delta'_{\mathrm{mf}} + \Delta_{\mathrm{xf}} + \Delta_{\mathrm{xm}}, \tag{3.2b}$$

which depend on the indices of the external particles a, b and the resonances i, j to which they are connected. Some of the indices i, j, a, b might be omitted if they do not appear in the considered subcontribution. Depending on whether the index b refers to the initial or final state, the contribution xf denotes either if or nf, and for the contribution xm either im or mn.

The matrix elements for diagrams of the type mm (Fig. 2i) and mf (Fig. 2e) are proportional to $\overline{Q}_i^2$ and $\overline{Q}_i Q_b$, respectively, so that we have used global charge conservation, Eq. (2.7), to fit them in the summation structure of Eq. (3.1). This is also the reason why their contributions appear in both Δ and Δ'. Furthermore the mf' contribution appears twice because we sum over $i < j$. The relations between the functions $\Delta_{\dots}$ and $\Delta'_{\dots}$ are

$$\Delta_{\mathrm{mm}}(i;j) = \Delta'_{\mathrm{mm}}(i) + \Delta'_{\mathrm{mm}}(j), \tag{3.3a}$$

$$\Delta_{\mathrm{mf}}(i,a;j,b) = \Delta'_{\mathrm{mf}}(i,a) + \Delta'_{\mathrm{mf}}(j,b), \tag{3.3b}$$

$$\Delta_{\mathrm{mf}'}(i,a;j,b) = \Delta'_{\mathrm{mf}'}(i;j,b) + \Delta'_{\mathrm{mf}'}(j;i,a), \tag{3.3c}$$

so that we only need to give the primed functions $\Delta'_{\dots}$.

The virtual parts of the not manifestly non-factorizable contributions are

$$\begin{aligned}\Delta_{\mathrm{mm}'} \sim\ & -\left(\overline{\overline{s}}_{ij} - M_i^2 - M_j^2\right)\Big\{C_0\left(\overline{k}_i^2, \overline{\overline{s}}_{ij}, \overline{k}_j, 0, \overline{M}_i^2, \overline{M}_j^2\right) \\ & \qquad - C_0\left(M_i^2, \overline{\overline{s}}_{ij}, M_j^2, m_\gamma^2, M_i^2, M_j^2\right)\Big\},\end{aligned} \tag{3.4a}$$

$$\Delta'_{\mathrm{mm}} \sim 2M_i^2\left\{\frac{B_0\left(\overline{k}_i^2, 0, \overline{M}_i^2\right) - B_0\left(\overline{M}_i^2, m_\gamma^2, \overline{M}_i^2\right)}{K_i} - B_0'\left(M_i^2, m_\gamma^2, M_i^2\right)\right\}, \tag{3.4b}$$

$$\begin{aligned}\Delta'_{\mathrm{mf}} \sim\ & -(\tilde{s}_{ia} - M_i^2 - m_a^2)\Big\{C_0\left(\overline{k}_i^2, \tilde{s}_{ia}, m_a^2, 0, \overline{M}_i^2, m_a^2\right) \\ & \qquad - C_0\left(M_i^2, \tilde{s}_{ia}, m_a^2, m_\gamma^2, M_i^2, m_a^2\right)\Big\},\end{aligned} \tag{3.4c}$$

$$\begin{aligned}\Delta_{\mathrm{xm}} \sim\ & -\left(\overline{s}_{ib} - M_i^2 - m_b^2\right)\Big\{C_0\left(\overline{k}_i^2, \overline{s}_{ib}, m_b^2, 0, \overline{M}_i^2, m_b^2\right) \\ & \qquad - C_0\left(M_i^2, \overline{s}_{ib}, m_b^2, m_\gamma^2, M_i^2, m_b^2\right)\Big\}.\end{aligned} \tag{3.4d}$$

The parts in curly brackets contain the subtraction of the respective factorizable parts which are obtained by setting the virtualities of the resonances on their real masses before the loop integration, as discussed in Sec. 2.2.3.

The manifestly non-factorizable virtual contributions read

$$\Delta_{\mathrm{ff}'} \sim -(s_{ab} - m_a^2 - m_b^2) K_i K_j E_0\left(k_a, \overline{k}_i, -\overline{k}_j, -k_b, m_\gamma^2, m_a^2, \overline{M}_i^2, \overline{M}_j^2, m_b^2\right), \tag{3.5a}$$

$$\Delta'_{\mathrm{mf}'} \sim -(\overline{s}_{ib} - M_i^2 - m_b^2) K_j D_0\left(\overline{k}_i, -\overline{k}_j, -k_b, m_\gamma^2, \overline{M}_i^2, \overline{M}_j^2, m_b^2\right), \tag{3.5b}$$

$$\Delta_{\mathrm{xf}} \sim -(s_{ab} - m_a^2 - m_b^2) K_i D_0\left(k_a, \overline{k}_i, -k_b, m_\gamma^2, m_a^2, \overline{M}_i^2, m_b^2\right). \tag{3.5c}$$

These contributions do not have factorizable counterparts.

For the second sum in Eq. (3.1) it is instructive to write down an explicit expression, at least for the case of massless external particles. Using the loop integrals given in App. C for $m_a, m_b \to 0$, the function Δ' reads

$$\Delta' \sim 2\left[\ln\left(\frac{M_i^2-\widetilde{s}_{ia}}{M_i^2}\right)+\ln\left(\frac{M_i^2-\overline{s}_{ib}}{-s_{ab}}\right)-1\right]\ln\left(\frac{-K_i}{m_\gamma M_i}\right)+\mathcal{L}\mathrm{i}_2\left(\frac{M_i^2-\widetilde{s}_{ia}}{M_i^2},\frac{M_i^2-\overline{s}_{ib}}{-s_{ab}}\right)+2. \tag{3.6}$$

where s_{ab}, $\widetilde{s}_{ia}$, and $\overline{s}_{ib}$ are implicitly understood as $s_{ab}+\mathrm{i}0$, $\widetilde{s}_{ia}+\mathrm{i}0$, and $\overline{s}_{ib}+\mathrm{i}0$, respectively. The dilogarithmic function $\mathcal{L}\mathrm{i}_2$ is defined in Eq. (C.5).

The correction factor δ_{nfact} contains soft divergences which are regularized as terms proportional to $\ln m_\gamma$ (or poles $1/\epsilon$ in $D = 4 - 2\epsilon$ dimensions, cf. App. C). These terms always appear as logarithms $\ln[m_\gamma M_i/(\overline{M}_i^2 - \overline{k}_i^2)]$ as a result of the connection between the soft divergence in the loop integration and the resonance at $\overline{k}_i^2 = M_i^2$.

Note, however, that the whole correction factor δ_{nfact} is free of mass singularities of the external particles a, b if one or more masses m_a, m_b become small. In the subcontribution of Eq. (3.6), this is directly visible, but for the other contributions there is a non-trivial cancellation between the corresponding mass singularities that appear in individual contributions. For small masses m_a, m_b it is, thus, possible to set the masses to zero consistently, which changes individual singular loop integrals, but not the final result for δ_{nfact}. In view of the limits $K_i \to 0$, note that there are two different types of non-analytic terms: The mentioned $\ln K_i$ terms and rational functions of the form $K_iK_j/(aK_i^2 + bK_iK_j + cK_j^2)$ originating from the five-point functions of Eq. (3.5a), where a, b, c are polynomial in kinematical invariants. Terms of the latter type require at least two different resonances and already appeared in the treatment of the W-pair production [22, 23, 24, 15, 16, 41].

In order not to spoil the cancellation of mass singularities, it is essential to use a unique procedure to isolate the non-analytic terms in the limit $\overline{K}_i^2, \overline{M}_i^2 \to M_i^2$ and to perform the on-shell projection of the phase space in the regular terms.

Our results on photonic non-factorizable corrections confirm the generic results given in the appendix of Ref. [15], which were formulated for several resonances and non-resonant final-state particles as well, though without details on their derivation. The specific formulas of Ref. [15] are given for the situation where resonances decay into two massless particles, an assumption we do not make. Moreover, we have presented a detailed general derivation of the photonic non-factorizable corrections, including a definition of the underlying ESPA current.

3.2 Examples

3.2.1 Single Z- or W-boson production in hadronic collisions

The simplest application of Eq. (3.1) is the production of a single resonance, e.g. the Drell–Yan-like production $q\overline{q} \to \mathrm{Z} \to \ell^-\ell^+$ or $q\overline{q}' \to \mathrm{W}^\pm \to \nu_\ell\ell^+/\ell^-\overline{\nu}_\ell$. There is only one resonance ($r = i = 1$) and no additional non-resonant particles in the final state ($n = 0$), so that Eq. (3.1) simplifies to

$$\delta_{\mathrm{nfact}} = -\sum_{a\in R_1}\sum_{b\in I}\sigma_a Q_a \sigma_b Q_b \frac{\alpha}{\pi}\,\mathrm{Re}\left\{\Delta'\right\}. \tag{3.7}$$

Since the external fermion masses are negligible, we can make use of Δ' as given in Eq. (3.6). The relevant kinematical invariants read

$$\begin{aligned} s_{12} &= s_{34} = 2k_1 \cdot k_2 = \quad 2p_1 \cdot p_2 = s, \qquad \overline{s}_{11} = \overline{s}_{12} = 0, \\ s_{13} &= s_{24} = 2k_1 \cdot k_3 = -2p_1 \cdot k_3 = t, \qquad \widetilde{s}_{13} = \widetilde{s}_{14} = 0, \\ s_{14} &= s_{23} = 2k_1 \cdot k_4 = -2p_1 \cdot k_4 = u, \end{aligned} \tag{3.8}$$

where we have taken the numbering $I = \{1,2\}$, $R_1 = \{3,4\}$ and s,t,u are the usual Mandelstam variables. With the particle ordering defined above, the sign factors σ_a are

$$\sigma_1 = -\sigma_2 = 1, \quad \sigma_3 = -\sigma_4 = -1. \tag{3.9}$$

For the case of $\mathrm{W}^\pm$ production/decay, the charge assignment is

$$Q_1 = Q_\mathrm{u}, \quad Q_2 = Q_\mathrm{d}, \quad Q_3 = Q_\nu = 0, \quad Q_4 = Q_\ell = -1, \quad \overline{Q}_1 = Q_\mathrm{u} - Q_\mathrm{d}, \tag{3.10}$$

so that δ_nfact is given by

$$\begin{aligned} \delta_\mathrm{nfact} = -\frac{\alpha}{\pi}\Bigg\{ 2\left[1 - Q_\mathrm{u} \ln\left(-\frac{M_\mathrm{W}^2}{\hat{u}}\right) + Q_\mathrm{d} \ln\left(-\frac{M_\mathrm{W}^2}{\hat{t}}\right)\right] \ln\left(\frac{\overline{M}_\mathrm{W}^2 - s}{m_\gamma M_\mathrm{W}}\right) \\ - Q_\mathrm{u}\,\mathrm{Li}_2\left(1 + \frac{M_\mathrm{W}^2}{\hat{u}}\right) + Q_\mathrm{d}\,\mathrm{Li}_2\left(1 + \frac{M_\mathrm{W}^2}{\hat{t}}\right) - 2\Bigg\}, \end{aligned} \tag{3.11}$$

where we have made the difference between the Mandelstam variables and their on-shell-projected counterparts $\hat{t}, \hat{u}$ explicit. For a single resonance with only massless external particles, an appropriate on-shell projection can be simply realized by the rescaling

$$s \to \frac{M_\mathrm{W}^2}{s}\, s = M_\mathrm{W}^2, \quad t \to \frac{M_\mathrm{W}^2}{s}\, t = \hat{t}, \quad u \to \frac{M_\mathrm{W}^2}{s}\, u = \hat{u}. \tag{3.12}$$

This result for δ_nfact agrees with the one given for the case of W^+ production in Eq. (2.22) of Ref. [17].

For Z-boson production the charges are given by

$$Q_1 = Q_2 = Q_q, \quad Q_3 = Q_4 = Q_\ell = -1, \quad \overline{Q}_1 = 0. \tag{3.13}$$

The resonance is neutral, so that the contributions mm, mf, and im vanish, and the result can be written as

$$\delta_\mathrm{nfact} = -\sum_{a=3,4}\sum_{b=1,2} \sigma_a Q_a \sigma_b Q_b \frac{\alpha}{\pi}\left\{ 2\ln\left(\frac{M_\mathrm{Z}^2}{-\hat{s}_{ab}}\right) \ln\left(\frac{\overline{M}_\mathrm{Z}^2 - s}{m_\gamma M_\mathrm{Z}}\right) + \mathrm{Li}_2\left(1 + \frac{M_\mathrm{Z}^2}{\hat{s}_{ab}}\right)\right\}, \tag{3.14}$$

where again $\hat{s}_{ab}$ results from s_{ab} by the on-shell projection (3.12) in accordance with Eq. (2.9) of Ref. [18].

3.2.2 W-pair production in lepton/hadron/photon collisions

For the case of $\overline{f}_1 f_2 \to \mathrm{W}^+\mathrm{W}^- \to f_3\overline{f}_4 f_5\overline{f}_6$, we choose the index sets appearing in Eq. (3.1) to be

$$I = \{1,2\}, \quad R_1 = \{3,4\}, \quad R_2 = \{5,6\}, \quad N = \emptyset. \tag{3.15}$$

The corresponding sign factors are

$$\sigma_1 = -1, \quad \sigma_2 = 1, \quad \sigma_3 = -1, \quad \sigma_4 = 1, \quad \sigma_5 = -1, \quad \sigma_6 = 1 \tag{3.16}$$

and therefore $r = 2$ and $n = 0$. $N = \emptyset$ means there are no additional non-resonant particles, so that the sum over b in Eq. (3.1) simply runs over the initial-state particles. Furthermore, since $\overline{f}_1$ is the antiparticle of f_2, we have $\sum_{b\in I}\sigma_b Q_b = 0$, so that the contributions from Δ'_{mm} and Δ'_{mf} cancel in Δ' given in Eq. (3.2b), because they do not depend on b.

The initial-state contributions, i.e. the function $\Delta'(i,a;b) = \Delta_{\mathrm{xm}}(i,a;b) + \Delta_{\mathrm{xf}}(i,a;b)$, can be brought into a form that can be summed together with the remaining non-vanishing contributions, Δ. To this end, we first define the relative charge of the initial-state fermions $Q_f = Q_1 = Q_2$ and express their sign factors $\sigma_{1,2}$ in terms of the charges of the vector bosons,

$$\sigma_1 = -\sigma_2 = \sum_{c\in R_1}\sigma_c Q_c = -\sum_{c\in R_2}\sigma_c Q_c, \tag{3.17}$$

and then explicitly perform the summation over i and b, i.e.

$$\sum_{i=1}^{2}\sum_{a\in R_i}\sum_{b\in I}\sigma_a Q_a \sigma_b Q_b \mathrm{Re}\{\Delta'(i,a;b)\} = \sum_{a\in R_1}\sum_{c\in R_2}\sigma_a Q_a \sigma_c Q_c (-Q_f)\mathrm{Re}\left\{\Delta'_{\mathrm{im}}(a;c) + \Delta'_{\mathrm{if}}(a;c)\right\}. \tag{3.18}$$

On the r.h.s. of Eq. (3.18) we defined two new functions, one of them

$$\begin{aligned}\Delta'_{\mathrm{im}}(a;c) = \quad & \Delta_{\mathrm{im}}(i=1,a;b=1) - \Delta_{\mathrm{im}}(i=1,a;b=2) \\ & - \Delta_{\mathrm{im}}(i=2,c;b=1) + \Delta_{\mathrm{im}}(i=2,c;b=2),\end{aligned} \tag{3.19}$$

in which the summation over i and b is explicit. The definition of Δ'_{if} is analogous.

As previously constructed, the remaining contributions Δ have the same summation structure as the r.h.s. of Eq. (3.18), because $i = 1$ and $j = 2$, so that with the identity $\sigma_a\sigma_b = (-1)^{a+b}$ Eq. (3.1) reads

$$\delta_{\mathrm{nfact}} = \sum_{a\in R_1}\sum_{b\in R_2}(-1)^{a+b+1}Q_a Q_b \frac{\alpha}{\pi}\mathrm{Re}\left\{\Delta''\right\}, \tag{3.20}$$

where we collected all contributions in

$$\Delta'' = \Delta_{\mathrm{mm}} + \Delta_{\mathrm{mf}} + \Delta_{\mathrm{mm}'} + \Delta_{\mathrm{mf}'} + \Delta_{\mathrm{ff}'} - Q_f\left(\Delta'_{\mathrm{if}} + \Delta'_{\mathrm{im}}\right). \tag{3.21}$$

An on-shell projection is given in Sec. 2.2.2. Here we specialize to the case of two W bosons and give the on-shell-projected momenta $\hat{k}_i$ in the centre-of-mass frame. The initial-state momenta are unmodified,

$$\hat{k}_1 = k_1, \quad \hat{k}_2 = k_2, \tag{3.22}$$

implying $\bar{\bar{s}}_{12} = s$. Since $M_1 = M_2 = M_\mathrm{W}$ the triangle function is $\lambda = s^2\beta^2$ with the velocity $\beta = \sqrt{1 - 4M_\mathrm{W}^2/s}$. Using the momenta given in Eq. (2.14) and fixing the direction $\boldsymbol{e}_1 = \overline{\boldsymbol{k}}_1/|\overline{\boldsymbol{k}}_1|$ of the W^+ boson, leads to

$$\hat{\bar{k}}_1 = \frac{1}{2}\sqrt{s}\,(1, \beta\boldsymbol{e}_1)\,, \qquad \hat{\bar{k}}_2 = -\hat{k}_1 - \hat{k}_2 - \hat{\bar{k}}_1. \tag{3.23}$$

Using Eq. (2.15) and making use of the fact that the fermions are massless, the on-shell projection reduces to a scale factor for the momentum whose direction we want to preserve. Since scaling massless momenta commutes with boosts, the scale factor is an invariant and can be easily computed in the centre-of-mass frame of the vector boson,

$$\hat{k}_3 = k_3 \frac{M_\mathrm{W}^2}{2\hat{\bar{k}}_1 k_3}, \qquad \hat{k}_4 = \hat{\bar{k}}_1 - \hat{k}_3, \tag{3.24a}$$

$$\hat{k}_5 = k_5 \frac{M_\mathrm{W}^2}{2\hat{\bar{k}}_2 k_5}, \qquad \hat{k}_6 = \hat{\bar{k}}_2 - \hat{k}_6, \tag{3.24b}$$

where the scale factors are derived from the conditions $\hat{k}_4^2 = \hat{k}_6^2 = 0$. These momenta must be inserted into Eqs. (3.4) and (3.5) which simplifies some of the kinematical prefactors, e.g. $\bar{\bar{s}}_{12} \to s$ and $\tilde{s}_{ia} \to 0$, for all $a \in R_i$. These results agree for the case $\overline{f}_1 = \mathrm{e}^+, f_2 = \mathrm{e}^-, Q_f = -1$ with the one given in Refs. [24, 12] and for the case of initial-state quarks with Refs. [15, 16].

As already mentioned in Sec. 2.2.2, the chosen on-shell projection constitutes an intrinsic ambiguity on the method. To determine the error introduced by this ambiguity and to verify that the choice is suitable results obtained with different on-shell projections can be compared. For $\mathrm{e}^+\mathrm{e}^- \to \mathrm{WW} \to 4\,$fermions this check was carried out in Ref. [12], i.e. the results from the on-shell projection as defined above was compared against results where the direction of k_4 instead k_3 was preserved. The comparison revealed differences from changing the on-shell projections that are of the order of all other intrinsic uncertainties of the double-pole approximation (DPA), as expected.

For the case of two initial photons, $\gamma\gamma \to \mathrm{W}^+\mathrm{W}^-$, there are no initial-state contributions, i.e. $Q_f = Q_\gamma = 0$ in Eq. (3.21). Electroweak corrections to this process in DPA, including these non-factorizable corrections, were calculated in Ref. [41].

3.2.3 Vector-boson scattering at hadron colliders

A prominent process featuring the production of additional non-resonant particles that were absent in the two previous examples is the case of vector-boson scattering at hadron colliders. The production of two vector bosons that are able to scatter off each other is only possible via radiation off a quark or an antiquark line, which then subsequently form jets in the final state. We thus have, at the parton level, the processes $q_1q_2 \to VV'q_7q_8 \to \ell_3\overline{\ell}_4\ell_5\overline{\ell}_6q_7q_8$ and all possible combinations with antiquarks that are consistent with charge conservation. The index sets, thus, are

$$I = \{1, 2\}, \quad R_1 = \{3, 4\}, \quad R_2 = \{5, 6\}, \quad N = \{7, 8\}. \tag{3.25}$$

A particularly interesting process is the scattering of same-sign W bosons, because, e.g., the appearance of $\mu^\pm\mu^\pm$ pairs in an event is a rather clean event signature and the QCD-initiated production can be efficiently suppressed by cuts [42].

Although desirable to reach a precision of some percent, electroweak corrections to this process are are not yet available at this time, due to the fact that the full correction to a $2 \to 6$ process is extremely challenging. However, as we argue here, the full correction is also not necessary, because an evaluation of the corrections in DPA will certainly be good enough. In DPA, the vector-boson scattering is a $2 \to 4$ particle production process with two resonances followed by two vector-boson decays, so that the virtual factorizable corrections can be calculated with modern automated tools for one-loop amplitudes. The non-factorizable corrections can be evaluated using our master formula presented in Sec. 3 in a similar fashion as in the examples discussed in the previous sections.

The on-shell projection can be performed as given in Sec. 2.2.2. We then keep the momenta of the initial-state particles and also the momenta of the non-resonant final states, i.e.

$$\hat{k}_1 = k_1, \quad \hat{k}_2 = k_2, \quad \hat{k}_7 = k_7, \quad \hat{k}_8 = k_8. \tag{3.26}$$

In the centre-of-mass frame of the vector bosons, i.e. the frame where $\boldsymbol{k}_1+\boldsymbol{k}_2+\boldsymbol{k}_7+\boldsymbol{k}_8 = 0$, we can easily construct the momenta. If the vector bosons have the same mass M_V, the momenta are given by Eq. (3.23) if we make the replacements $s \to \overline{\overline{s}}_{12}$ and $M_\mathrm{W} \to M_V$. If they have different masses, e.g. in the case of $\mathrm{W}^\pm\mathrm{Z}$ scattering, we can use the general procedure as given in Eq. (2.15).

4 Conclusion

Many interesting particle processes at present and potential future high-energy colliders share the pattern of producing several unstable particles in intermediate resonant states which decay subsequently, thereby producing final states of high multiplicities. At run 2 of the LHC, which has started in 2015, multiple-vector-boson production such as $\mathrm{pp} \to \mathrm{WWW} \to 6$ leptons and massive vector-boson scattering such as $\mathrm{pp} \to \mathrm{WW} + 2$ jets $\to$ 4 leptons + 2 jets are prominent examples for corresponding upcoming analyses in the electroweak sector. In spite of the smaller cross sections of high-multiplicity processes, predictions for those processes nevertheless have to include radiative corrections of the strong and electroweak interactions at next-to-leading order, in order to reach a precision of about 10%, or better since both types of corrections are generically of this size or even larger in the TeV range.

Calculating radiative corrections to resonance processes poses additional complications on top of the usual complexity of higher-order calculations, since gauge invariance is jeopardized by the necessary Dyson summation of the resonance propagators. For low and intermediate multiplicities, complete next-to-leading-order calculations are feasible within the complex-mass scheme, but unnecessarily complicated and also not needed in view of precision for high multiplicities. In those cases, predictions where matrix elements are based on expansions about resonance poles are adequate. Such expansions can be based on scattering amplitudes directly or on specifically designed effective field theories. If only the leading contribution of the expansion is kept, the approach—known as pole

approximation—is particularly intuitive. At next-to-leading order, corrections are classified into separately gauge-invariant factorizable and non-factorizable corrections, where the former can be attributed to the production and decay of the unstable particles on their mass shell. The remaining non-factorizable corrections are induced by the exchange of soft photons or gluons between different production and decay subprocesses.

In this paper, we have presented explicit analytical results for the non-factorizable photonic virtual corrections to processes involving an arbitrary number of unstable particles at the one-loop level. The results represent an essential building block in the calculation of next-to-leading-order electroweak corrections in pole approximation and are ready for a direct implementation in computer codes. As illustrating examples, we have rederived known results for the single and pair production of electroweak gauge bosons and have outlined the approach for vector-boson scattering.

A generalization of the results to QCD corrections is straightforward and merely requires the inclusion of the colour flow in the algebraic parts of the individual contributions, while the analytic part containing the loop integrals remains the same.

The presented results on virtual non-factorizable corrections help to close a gap in the ongoing effort of several groups towards the fully automated calculation of next-to-leading-order corrections, since the automation of the remaining virtual factorizable corrections is well under control within QCD with up to 4–6 final-state particles and becomes more and more mature for electroweak corrections as well. The situation in view of real QCD and real photonic electroweak corrections is even better, since tree-level calculations with up to about 10 final-state particles based on full matrix elements are possible with modern multi-purpose Monte Carlo generators. Having at hand generic results on virtual non-factorizable corrections, thus, opens the door to the fully automated calculation of virtual corrections to resonance processes in pole approximation.

Acknowledgements

We thank Ansgar Denner for carefully reading the manuscript, and C.S. is grateful to Christian Schwinn for useful discussions on non-factorizable corrections. This work is supported by the German Science Foundation (DFG) under contract Di 784/3-1 and via the Research Training Group GRK 2044.

Appendix

A Soft-photon emission off resonances

In this appendix we derive Eqs. (2.21a) and (2.21b), which describe soft-photon emission off a resonating particle, for particles of spin 0, 1/2, or 1. Obviously it is sufficient to prove only the first of these equations; the second follows from the first upon replacing the momentum $\overline{k}_i \to \overline{k}_i - q$, taking into account that the photon momentum q is negligible in the numerator.

If the radiating particle i has spin 0, the proof is extremely simple. Inserting the Feynman rule for the coupling of a scalar particle i to a photon and for the two scalar propagators, the subdiagram on the l.h.s. of Eq. (2.21a) can be directly brought to the desired form,

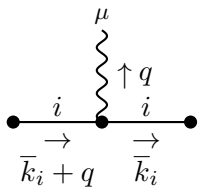

$$= \frac{\mathrm{i}}{K_i(q)} (-\mathrm{i}e\overline{Q}_i) \left(2\overline{k}_i + q\right)^\mu \frac{\mathrm{i}}{K_i} \sim \frac{2e\overline{Q}_i \overline{k}_i^\mu}{K_i(q)} \times$$

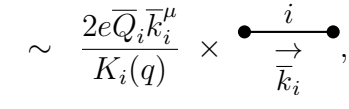

, (A.1)

where $\sim$ means that the two sides later produce the same soft singularity structure for small photon momentum q when embedded in a full diagram. According to the arguments of Sec. 2.3.1, the calculated loop diagram changes by this approximation only in terms that are not enhanced by resonance i. In Eq. (A.1) the necessary approximation was just to omit q in the numerator.

If i is a spin-1/2 fermion, inserting the relevant Feynman rules produces

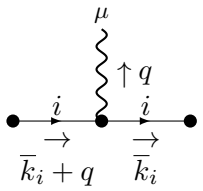

$$= \frac{\mathrm{i}\left(\overline{\not{k}} + \overline{M}_i\right)}{K_i} (-\mathrm{i}e\overline{Q}_i)\gamma^\mu \frac{\mathrm{i}\left(\overline{\not{k}} + \not{q} + \overline{M}_i\right)}{K_i(q)}. \quad (A.2)$$

A simple rearrangement of the Dirac matrices leads to the desired form after dropping again irrelevant (non-resonant) terms,

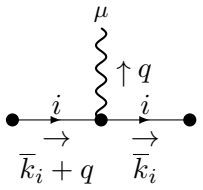

$$\sim \mathrm{i}e\overline{Q}_i \frac{\left(\overline{\not{k}}_i + \overline{M}_i\right)\gamma^\mu\left(\overline{\not{k}}_i + \overline{M}_i\right)}{K_i(q)K_i} = \mathrm{i}e\overline{Q}_i \frac{2\overline{k}_i^\mu\left(\overline{\not{k}}_i + \overline{M}_i\right) - K_i}{K_i(q)K_i}$$

$$\sim \frac{2e\overline{Q}_i\overline{k}_i^\mu}{K_i(q)} \times$$

. (A.3)

Analogous manipulations with the opposite fermion flow for an antifermion resonance produce the same result.

The case where i is a charged spin-1 boson deserves more care. We assume that i is a gauge boson that receives its mass by the Higgs mechanism, just like the W boson in the SM. In principle, we, thus, have to consider all possible loop diagrams with subdiagrams (2.21a), in which the resonance line i represents the gauge-boson field, its corresponding would-be Goldstone boson, or even a Faddeev–Popov ghost field. However, if we switch to an R_ξ gauge for the i field where its gauge parameter $\xi_i \neq 1$, the propagators of the corresponding Goldstone and ghost fields develop their pole at $\overline{k}_i^2 = \xi_i\overline{M}_i^2 \neq \overline{M}_i^2$. However, a pole at $\overline{k}_i^2 = \overline{M}_i^2$ would be necessary to produce soft divergences on resonance which in turn is a necessary condition for the corresponding diagrams to contribute to non-factorizable corrections. Consequently, we can ignore subgraphs (2.21a) with would-be

Goldstone boson or ghost fields in the following. In the adopted R_ξ gauge the i propagator is given by

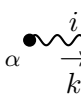

$$= G_{i,\alpha\beta}(k) = \frac{-\mathrm{i}\left(g_{\alpha\beta} - \frac{k_\alpha k_\beta}{k^2}\right)}{k^2 - \overline{M}_i^2} + \frac{-\mathrm{i}\xi_i \frac{k_\alpha k_\beta}{k^2}}{k^2 - \xi_i \overline{M}_i^2}. \tag{A.4}$$

Obviously the second term with the unphysical pole at $\overline{k}_i^2 = \xi_i \overline{M}_i^2$ again does not contribute to the non-factorizable corrections and can be ignored. Inserting the respective Feynman rules, we obtain

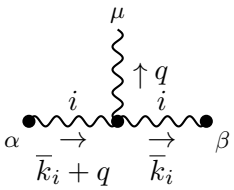

$$\begin{aligned}
&= (-\mathrm{i}\overline{Q}_i e)\left[g^{\mu\nu}\left(\overline{k}_i + 2q\right)^\rho + g^{\nu\rho}\left(-2\overline{k}_i - q\right)^\mu + g^{\rho\mu}\left(\overline{k}_i - q\right)^\nu\right] \\
&\quad \times G_{i,\alpha\nu}\left(\overline{k}_i + q\right) G_{i,\rho\beta}\left(\overline{k}_i\right) \\
&\sim \mathrm{i}\overline{Q}_i e\left[g^{\mu\nu}\overline{k}_i^\rho - 2g^{\nu\rho}\overline{k}_i^\mu + g^{\rho\mu}\overline{k}_i^\nu\right] \frac{g_{\alpha\nu} - \frac{\overline{k}_{i,\alpha}\overline{k}_{i,\nu}}{\overline{k}_i^2}}{K_i(q)} \frac{g_{\rho\beta} - \frac{\overline{k}_{i,\rho}\overline{k}_{i,\beta}}{\overline{k}_i^2}}{K_i} \\
&= -2\mathrm{i}\overline{Q}_i e \overline{k}_i^\mu \frac{g_{\alpha\beta} - \frac{\overline{k}_{i,\alpha}\overline{k}_{i,\beta}}{\overline{k}_i^2}}{K_i(q) K_i} \\
&\sim \frac{2e\overline{Q}_i \overline{k}_i^\mu}{K_i(q)} \times
\end{aligned}$$

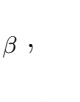

, (A.5)

where we have neglected q in the numerator in the first $\sim$ relation and performed simple four-vector contractions in the subsequent step. The final $\sim$ relation, which proves Eq. (2.21a), is again valid up to irrelevant terms with an unphysical propagator pole.

B Derivation of virtual non-factorizable corrections

In this appendix we calculate the non-factorizable corrections induced by the various diagram types shown in Fig. 2, making use of the generic results derived in Sec. 2.3, which are summarized in Eq. (2.29). Our aim is to express all contributions in terms of known standard scalar one-loop integrals as defined in App. C.

List of the different types of non-factorizable corrections:

- The *ff′*-diagram in Fig. 2a is manifestly non-factorizable and involves the following combination of currents

$$j_a(q) \cdot j_b(-q) = \frac{2e\sigma_a Q_a k_a^\mu}{q^2 + 2qk_a} \frac{K_i}{K_i(q)} \frac{2e\sigma_b Q_b k_{b,\mu}}{q^2 - 2qk_b} \frac{K_j}{K_j(-q)}, \tag{B.1}$$

  where $a \in R_i$ and $b \in R_j$ are decay particles of two different resonances $i, j \in \overline{R}$, $i \neq j$. Inserting this into the integral (2.29) and using $e^2 = 4\pi\alpha$, directly leads to the contribution $\delta_{\mathrm{ff}'}(i,a;j,b) = -\frac{\alpha}{\pi}\sigma_a Q_a \sigma_b Q_b \,\mathrm{Re}\left\{\Delta_{\mathrm{ff}'}(i,a;j,b)\right\}$ with

$$\begin{aligned}
\Delta_{\mathrm{ff}'}(i,a;j,b) &= -\left(s_{ab} - m_a^2 - m_b^2\right) K_i K_j \\
&\quad \times E_0(k_a, \overline{k}_i, -\overline{k}_j, -k_b, m_\gamma^2, m_a^2, \overline{M}_i^2, \overline{M}_j^2, m_b^2).
\end{aligned} \tag{B.2}$$

The sum over all non-equivalent pairs i, j and corresponding pairs a, b is

$$\delta_{\mathrm{ff}'} = -\frac{\alpha}{\pi} \sum_{i=1}^{r} \sum_{j=i+1}^{r} \sum_{a \in R_i} \sum_{b \in R_j} \sigma_a Q_a \sigma_b Q_b \,\mathrm{Re}\left\{\Delta_{\mathrm{ff}'}(i,a;j,b)\right\}. \tag{B.3}$$

- The *xf*-diagrams in Fig. 2b and Fig. 2c are manifestly non-factorizable and involve the following combination of currents,

$$j_a(q) \cdot j_b(-q) = \frac{2e\sigma_a Q_a k_a^\mu}{q^2 + 2qk_a} \frac{K_i}{K_i(q)} \frac{2e\sigma_b Q_b k_{b,\mu}}{q^2 - 2qk_b}, \tag{B.4}$$

where $a \in R_i$, $i \in \overline{R}$ and $b \in I \cup N$. Inserting this into the integral (2.29), directly leads to the contribution $\delta_{\mathrm{xf}}(i,a;b) = -\frac{\alpha}{\pi}\sigma_a Q_a \sigma_b Q_b \,\mathrm{Re}\left\{\Delta_{\mathrm{xf}}(i,a;b)\right\}$ with

$$\begin{aligned}
\Delta_{\mathrm{xf}}(i,a;b) &= -(s_{ab} - m_a^2 - m_b^2)\, K_i\, D_0(k_a, \overline{k}_i, -k_b, m_\gamma^2, m_a^2, \overline{M}_i^2, m_b^2) \\
&= -(s_{ab} - m_a^2 - m_b^2)\, K_i\, D_0(m_a^2, \widetilde{s}_{ia}, \overline{s}_{ib}, m_b^2, \overline{k}_i^2, s_{ab}, m_\gamma^2, m_a^2, \overline{M}_i^2, m_b^2).
\end{aligned} \tag{B.5}$$

The sum over all resonances i and corresponding pairs a, b is

$$\delta_{\mathrm{xf}} = -\frac{\alpha}{\pi} \sum_{i=1}^{r} \sum_{a \in R_i} \sum_{b \in I \cup N} \sigma_a Q_a \sigma_b Q_b \,\mathrm{Re}\left\{\Delta_{\mathrm{xf}}(i,a;b)\right\}. \tag{B.6}$$

- The *mf′*-diagram in Fig. 2d is manifestly non-factorizable and receives contributions from the following combination of currents,

$$\begin{aligned}
\overline{j}_{\mathrm{in},i}(q) \cdot j_b(-q) + \overline{j}_{\mathrm{out},i}(q) \cdot j_b(-q) &= \frac{2e\overline{Q}_i \overline{k}_i^\mu}{q^2 + 2\overline{k}_i q} \left(\frac{K_i}{K_i(q)} - 1\right) \frac{2e\sigma_b Q_b k_{b,\mu}}{q^2 - 2qk_b} \frac{K_j}{K_j(-q)} \\
&= -\frac{4e^2 \overline{Q}_i \sigma_b Q_b\, \overline{k}_i \cdot k_b\, K_j}{K_i(q)(q^2 - 2qk_b) K_j(-q)},
\end{aligned} \tag{B.7}$$

where $i, j \in \overline{R}$ are different resonances ($i \neq j$) and $b \in R_j$. Inserting this into the integral (2.29), leads to the contribution $\delta_{\mathrm{mf}'}(i;j,b) = \frac{\alpha}{\pi}\overline{Q}_i \sigma_b Q_b \,\mathrm{Re}\left\{\Delta'_{\mathrm{mf}'}(i;j,b)\right\}$ with

$$\begin{aligned}
\Delta'_{\mathrm{mf}'}(i;j,b) &= -(\overline{s}_{ib} - \overline{k}_i^2 - m_b^2)\, K_j\, D_0(\overline{k}_i, -\overline{k}_j, -k_b, m_\gamma^2, \overline{M}_i^2, \overline{M}_j^2, m_b^2) \\
&\sim -(\overline{s}_{ib} - M_i^2 - m_b^2)\, K_j\, D_0(\overline{k}_i, -\overline{k}_j, -k_b, m_\gamma^2, \overline{M}_i^2, \overline{M}_j^2, m_b^2) \\
&= -(\overline{s}_{ib} - M_i^2 - m_b^2)\, K_j\, D_0(\overline{k}_i^2, \overline{\overline{s}}_{ij}, \widetilde{s}_{jb}, m_b^2, \overline{k}_j^2, \overline{s}_{ib}, m_\gamma^2, \overline{M}_i^2, \overline{M}_j^2, m_b^2).
\end{aligned} \tag{B.8}$$

The sum over the resonances i and j and its decay product b is

$$\begin{aligned}
\delta_{\mathrm{mf}'} &= \frac{\alpha}{\pi} \sum_{i=1}^{r} \sum_{\substack{j=1 \\ j \neq i}}^{r} \sum_{b \in R_j} \overline{Q}_i \sigma_b Q_b \,\mathrm{Re}\left\{\Delta'_{\mathrm{mf}'}(i;j,b)\right\} \\
&= -\frac{\alpha}{\pi} \sum_{i=1}^{r} \sum_{j=i+1}^{r} \sum_{a \in R_i} \sum_{b \in R_j} \sigma_a Q_a \sigma_b Q_b \Big(\mathrm{Re}\left\{\Delta'_{\mathrm{mf}'}(i;j,b)\right\} + \mathrm{Re}\left\{\Delta'_{\mathrm{mf}'}(j;i,a)\right\}\Big).
\end{aligned} \tag{B.9}$$

- The *mf*-diagram in Fig. 2e is not manifestly non-factorizable, since it contains a factorizable part. The non-factorizable part receives contributions from the following combination of currents,

$$\begin{aligned}\widetilde{j}_{\mathrm{out},i}(q)\cdot j_a(-q) &= \frac{2e\overline{Q}_i\overline{k}_i^{\mu}}{q^2-2\overline{k}_i q}\,\frac{2e\sigma_a Q_a k_{a,\mu}}{q^2-2qk_a}\,\frac{K_i}{K_i(-q)}\\ &= \frac{4e^2\overline{Q}_i\sigma_a Q_a\,\overline{k}_i\cdot k_a}{q^2-2qk_a}\left(\frac{1}{q^2-2\overline{k}_i q}-\frac{1}{K_i(-q)}\right),\end{aligned} \tag{B.10}$$

where $i\in\overline{R}$ and $a\in R_i$. Inserting this into the integral (2.29), leads to the contribution $\delta_{\mathrm{mf}}(i;a)=-\frac{\alpha}{\pi}\overline{Q}_i\sigma_a Q_a\,\mathrm{Re}\,\{\Delta'_{\mathrm{mf}}(i;a)\}$ with

$$\begin{aligned}\Delta'_{\mathrm{mf}}(i;a) &= (\tilde{s}_{ia}-\overline{k}_i^2-m_a^2)\Big\{C_0(-\overline{k}_i,-k_a,m_\gamma^2,\overline{k}_i^2,m_a^2)\\ &\qquad\qquad -C_0(-\overline{k}_i,-k_a,m_\gamma^2,\overline{M}_i^2,m_a^2)\Big\}\\ &\sim (\tilde{s}_{ia}-M_i^2-m_a^2)\Big\{C_0(M_i^2,\tilde{s}_{ia},m_a^2,m_\gamma^2,M_i^2,m_a^2)\\ &\qquad\qquad -C_0(\overline{k}_i^2,\tilde{s}_{ia},m_a^2,0,\overline{M}_i^2,m_a^2)\Big\},\end{aligned} \tag{B.11}$$

with the usual difference between the full off-shell diagram and its factorizable part with $\overline{k}_i^2=M_i^2$. The final form, where invariants are used as arguments of the C_0 integrals, makes the appearance of off-shell and on-shell momenta on the resonance lines better visible. The sum over all resonances i and its decay products a is

$$\begin{aligned}\delta_{\mathrm{mf}} &= -\frac{\alpha}{\pi}\sum_{i=1}^{r}\sum_{a\in R_i}\overline{Q}_i\sigma_a Q_a\,\mathrm{Re}\,\{\Delta'_{\mathrm{mf}}(i,a)\}\\ &= -\frac{\alpha}{\pi}\sum_{i=1}^{r}\sum_{a\in R_i}\left(\sum_{\substack{j=1\\ j\neq i}}^{r}\sum_{b\in R_j}+\sum_{b\in I\cup N}\right)\sigma_a Q_a\sigma_b Q_b\,\mathrm{Re}\,\{\Delta'_{\mathrm{mf}}(i,a)\}\\ &= -\frac{\alpha}{\pi}\sum_{i=1}^{r}\sum_{j=i+1}^{r}\sum_{a\in R_i}\sum_{b\in R_j}\sigma_a Q_a\sigma_b Q_b\Big(\mathrm{Re}\,\{\Delta'_{\mathrm{mf}}(i,a)\}+\mathrm{Re}\,\{\Delta'_{\mathrm{mf}}(j,b)\}\Big)\\ &\quad -\frac{\alpha}{\pi}\sum_{i=1}^{r}\sum_{a\in R_i}\sum_{b\in I\cup N}\sigma_a Q_a\sigma_b Q_b\,\mathrm{Re}\,\{\Delta'_{\mathrm{mf}}(i,a)\}\,.\end{aligned} \tag{B.12}$$

- The *xm*-diagrams in Fig. 2f and Fig. 2g are not manifestly non-factorizable, since they contain factorizable contributions as well. The non-factorizable part receives contributions from the following combination of currents,

$$\begin{aligned}\overline{j}_{\mathrm{in},i}(q)\cdot j_b(-q) &= \frac{2e\overline{Q}_i\overline{k}_i^{\mu}}{q^2+2\overline{k}_i q}\,\frac{K_i}{K_i(q)}\,\frac{2e\sigma_b Q_b k_{b,\mu}}{q^2-2qk_b}\\ &= \frac{4e^2\overline{Q}_i\sigma_b Q_b\,\overline{k}_i\cdot k_b}{q^2-2qk_b}\left(\frac{1}{q^2+2\overline{k}_i q}-\frac{1}{K_i(q)}\right),\end{aligned} \tag{B.13}$$

where $i \in \overline{R}$ and $b \in I \cup N$. Inserting this into the integral (2.29), leads to the contribution $\delta_{\rm xm}(i;b) = \frac{\alpha}{\pi}\overline{Q}_i\sigma_b Q_b \,\mathrm{Re}\,\{\Delta_{\rm xm}(i;b)\}$ with

$$\begin{aligned}\Delta_{\rm xm}(i;b) &= (\overline{s}_{ib} - \overline{k}_i^2 - m_b^2)\Big\{C_0(\overline{k}_i, -k_b, m_\gamma^2, \overline{k}_i^2, m_b^2) \\ &\qquad\qquad - C_0(\overline{k}_i, -k_b, m_\gamma^2, \overline{M}_i^2, m_b^2)\Big\} \\ &\sim (\overline{s}_{ib} - M_i^2 - m_b^2)\Big\{C_0(M_i^2, \overline{s}_{ib}, m_b^2, m_\gamma^2, M_i^2, m_b^2) \\ &\qquad\qquad - C_0(\overline{k}_i^2, \overline{s}_{ib}, m_b^2, 0, \overline{M}_i^2, m_b^2)\Big\},\end{aligned} \tag{B.14}$$

which again reflects the subtraction of the factorizable part with an on-shell momentum of the resonance ($\overline{k}_i^2 = M_i^2$) from the full off-shell diagram. The sum over all resonances i and other particles b of the production process reads

$$\begin{aligned}\delta_{\rm xm} &= \frac{\alpha}{\pi}\sum_{i=1}^{r}\sum_{b\in I\cup N}\overline{Q}_i\sigma_b Q_b\,\mathrm{Re}\,\{\Delta_{\rm xm}(i;b)\} \\ &= -\frac{\alpha}{\pi}\sum_{i=1}^{r}\sum_{a\in R_i}\sum_{b\in I\cup N}\sigma_a Q_a\sigma_b Q_b\,\mathrm{Re}\,\{\Delta_{\rm xm}(i;b)\}\,.\end{aligned} \tag{B.15}$$

- The mm'-diagram in Fig. 2h is not manifestly non-factorizable, i.e. it contains both factorizable and non-factorizable parts. Its non-factorizable contribution involves the following combinations of ESPA currents,

$$\begin{aligned}&\overline{j}_{{\rm out},i}(q)\cdot\overline{j}_{{\rm in},j}(-q) + \overline{j}_{{\rm in},i}(q)\cdot\overline{j}_{{\rm out},j}(-q) + \overline{j}_{{\rm in},i}(q)\cdot\overline{j}_{{\rm in},j}(-q) \\ &\quad= -\frac{2e\overline{Q}_i\overline{k}_i^\mu}{q^2+2\overline{k}_i q}\frac{2e\overline{Q}_j\overline{k}_{j,\mu}}{q^2-2\overline{k}_j q}\frac{K_j}{K_j(-q)} - \frac{2e\overline{Q}_i\overline{k}_i^\mu}{q^2+2\overline{k}_i q}\frac{K_i}{K_i(q)}\frac{2e\overline{Q}_j\overline{k}_{j,\mu}}{q^2-2\overline{k}_j q} \\ &\qquad+\frac{2e\overline{Q}_i\overline{k}_i^\mu}{q^2+2\overline{k}_i q}\frac{K_i}{K_i(q)}\frac{2e\overline{Q}_j\overline{k}_{j,\mu}}{q^2-2\overline{k}_j q}\frac{K_j}{K_j(-q)} \\ &\quad= 4e^2\overline{Q}_i\overline{Q}_j(\overline{k}_i\cdot\overline{k}_j)\left(\frac{1}{K_i(q)}\frac{1}{K_j(-q)} - \frac{1}{q^2+2\overline{k}_i q}\frac{1}{q^2-2\overline{k}_j q}\right),\end{aligned} \tag{B.16}$$

where $i,j \in \overline{R}$ are different resonances, $i \neq j$. We have used Eqs. (2.22a) and (2.22b) to obtain the final form. Inserting this into Eq. (2.29), we obtain its contribution $\delta_{\rm mm'}(i;j) = -\frac{\alpha}{\pi}\overline{Q}_i\overline{Q}_j\,\mathrm{Re}\,\{\Delta_{\rm mm'}(i;j)\}$ to $\delta_{\rm nfact}$, where

$$\begin{aligned}\Delta_{\rm mm'}(i;j) &= -\left(\overline{\overline{s}}_{ij} - \overline{k}_i^2 - \overline{k}_j^2\right) \\ &\qquad\times\left\{C_0\left(\overline{k}_i, -\overline{k}_j, m_\gamma^2, \overline{M}_i^2, \overline{M}_j^2\right) - C_0\left(\overline{k}_i, -\overline{k}_j, m_\gamma^2, \overline{k}_i^2, \overline{k}_j^2\right)\right\} \\ &\sim -\left(\overline{\overline{s}}_{ij} - M_i^2 - M_j^2\right) \\ &\qquad\times\left\{C_0\left(\overline{k}_i^2, \overline{\overline{s}}_{ij}, \overline{k}_j^2, 0, \overline{M}_i^2, \overline{M}_j^2\right) - C_0\left(M_i^2, \overline{\overline{s}}_{ij}, M_j^2, m_\gamma^2, M_i^2, M_j^2\right)\right\},\end{aligned} \tag{B.17}$$

where $\sim$ again means identical up to non-resonant terms. The final form nicely shows how the subtraction of the factorizable part, where the resonance momenta $\overline{k}_{i,j}$ are

on shell, from the full diagram defines the non-factorizable contribution. Summing over all resonance pairs i, j and using charge conservation in the form (2.8), the full mm' contribution can be written as

$$\begin{aligned}\delta_{\mathrm{mm}'} &= -\frac{\alpha}{\pi}\sum_{i=1}^{r}\sum_{j=i+1}^{r}\overline{Q}_i\overline{Q}_j\,\mathrm{Re}\left\{\Delta_{\mathrm{mm}'}(i;j)\right\} \\ &= -\frac{\alpha}{\pi}\sum_{i=1}^{r}\sum_{j=i+1}^{r}\sum_{a\in R_i}\sum_{b\in R_j}\sigma_a Q_a \sigma_b Q_b\,\mathrm{Re}\left\{\Delta_{\mathrm{mm}'}(i;j)\right\}.\end{aligned} \tag{B.18}$$

- The mm-diagram in Fig. 2i deserves some particular care, since it should be considered in combination with its contribution to the mass renormalization counterterm of resonance i. According to the ESPA currents, the following combination of currents defines the non-factorizable contribution,

$$\begin{aligned}\widetilde{j}_{\mathrm{out},i}(q)\cdot\overline{j}_{\mathrm{in},i}(-q) &= \frac{2e\overline{Q}_i\overline{k}_i^{\mu}}{q^2-2\overline{k}_i q}\,\frac{2e\overline{Q}_i\overline{k}_{i,\mu}}{q^2-2\overline{k}_i q}\,\frac{K_i}{K_i(-q)} \\ &= 4e^2\overline{Q}_i^2\overline{k}_i^2\left(\frac{1}{K_iK_i(-q)}-\frac{1}{K_i(q^2-2\overline{k}_i q)}+\frac{1}{(q^2-2\overline{k}_i q)^2}\right)\end{aligned} \tag{B.19}$$

for all $i\in\overline{R}$. Inserting this into the integral (2.29), leads to the contribution $\delta_{\mathrm{mm}}(i) = \frac{\alpha}{\pi}\overline{Q}_i^2\,\mathrm{Re}\left\{\Delta'_{\mathrm{mm}}(i)\right\}$ with[6]

$$\begin{aligned}\Delta'_{\mathrm{mm}}(i) &= 2\overline{k}_i^2\left\{\frac{B_0\left(\overline{k}_i^2,m_\gamma^2,\overline{M}_i^2\right)-B_0\left(\overline{k}_i^2,m_\gamma^2,\overline{k}_i^2\right)}{K_i}-B_0'\left(\overline{k}_i^2,m_\gamma^2,\overline{k}_i^2\right)\right\} \\ &\sim 2M_i^2\left\{\frac{B_0\left(\overline{k}_i^2,0,\overline{M}_i^2\right)-B_0\left(\overline{M}_i^2,m_\gamma^2,\overline{M}_i^2\right)}{K_i}-B_0'\left(M_i^2,m_\gamma^2,M_i^2\right)\right\}.\end{aligned} \tag{B.20}$$

This final form can be interpreted in two different ways: Taking the first B_0 term as the full off-shell contribution, the second and third terms correspond to its on-shell subtraction to obtain its non-factorizable part. Performing the same subtraction for the corresponding counterterm contribution connected with the i self-energy, gives zero, because there is no issue with respect to interchanging limits in the loop integration, since the renormalization constants are always calculated first. The alternative interpretation is to consider the terms in the curly brackets as the full off-shell contribution of the photon-exchange diagram and the corresponding counterterms, where the last-but-one and the last terms correspond to the mass and wave-function renormalization of the i line in the on-shell renormalization scheme, respectively. By construction, in this scheme on-shell particles do not receive self-energy corrections, i.e. the factorizable part of the considered contribution in curly brackets is zero, in accordance with our result.

[6]The term $\propto 1/(q^2-2\overline{k}_i q)^2$ can be identified with the momentum derivative $B_0'(p_1^2,m_\gamma^2,m_1^2) = \partial B_0(p_1^2,m_\gamma^2,m_1^2)/\partial p_1^2$ by applying $\partial/\partial p_1^2 = 1/(2p_1^2)p_1^\mu\partial/\partial p_1^\mu$ as follows: $\partial[1/(q^2+2p_1q+p_1^2-m_1^2)]/\partial p_1^2 = -(qp_1+p_1^2)/(q^2+2p_1q+p_1^2-m_1^2)^2/p_1^2 \sim -1/(q^2+2p_1q+p_1^2-m_1^2)^2$.

Summation over all resonances i leads to

$$\begin{aligned}
\delta_{\rm mm} &= +\frac{\alpha}{\pi}\sum_{i=1}^{r}\overline{Q}_i^2\,\mathrm{Re}\left\{\Delta'_{\rm mm}(i)\right\} = -\frac{\alpha}{\pi}\sum_{i=1}^{r}\sum_{a\in R_i}\sigma_a Q_a\overline{Q}_i\,\mathrm{Re}\left\{\Delta'_{\rm mm}(i)\right\}\\
&= -\frac{\alpha}{\pi}\sum_{i=1}^{r}\sum_{a\in R_i}\left(\sum_{\substack{j=1\\ j\neq i}}^{r}\sum_{b\in R_j}+\sum_{b\in I\cup N}\right)\sigma_a Q_a\sigma_b Q_b\,\mathrm{Re}\left\{\Delta'_{\rm mm}(i)\right\}\\
&= -\frac{\alpha}{\pi}\sum_{i=1}^{r}\sum_{j=i+1}^{r}\sum_{a\in R_i}\sum_{b\in R_j}\sigma_a Q_a\sigma_b Q_b\Big(\mathrm{Re}\left\{\Delta'_{\rm mm}(i)\right\}+\mathrm{Re}\left\{\Delta'_{\rm mm}(j)\right\}\Big)\\
&\quad -\frac{\alpha}{\pi}\sum_{i=1}^{r}\sum_{a\in R_i}\sum_{b\in I\cup N}\sigma_a Q_a\sigma_b Q_b\,\mathrm{Re}\left\{\Delta'_{\rm mm}(i)\right\}.
\end{aligned}\tag{B.21}$$

C Scalar Integrals

The scalar integrals used in this paper are defined as

$$B_0\left(p_1,m_\gamma^2,m_1^2\right) = (2\pi\mu)^{4-D}\int\frac{\mathrm{d}^Dq}{\mathrm{i}\pi^2}\frac{1}{q^2-m_\gamma^2}\frac{1}{(q+p_1)^2-m_1^2},\tag{C.1a}$$

$$C_0\left(p_1,p_2,m_\gamma^2,m_1^2,m_2^2\right) = (2\pi\mu)^{4-D}\int\frac{\mathrm{d}^Dq}{\mathrm{i}\pi^2}\frac{1}{q^2-m_\gamma^2}\prod_{i=1}^{2}\frac{1}{(q+p_i)^2-m_i^2},\tag{C.1b}$$

$$D_0\left(p_1,p_2,p_3,m_\gamma^2,m_1^2,m_2^2,m_3^2\right) = (2\pi\mu)^{4-D}\int\frac{\mathrm{d}^Dq}{\mathrm{i}\pi^2}\frac{1}{q^2-m_\gamma^2}\prod_{i=1}^{3}\frac{1}{(q+p_i)^2-m_i^2},\tag{C.1c}$$

$$E_0\left(p_1,p_2,p_3,p_4,m_\gamma^2,m_1^2,m_2^2,m_3^2,m_4^2\right) = (2\pi\mu)^{4-D}\int\frac{\mathrm{d}^Dq}{\mathrm{i}\pi^2}\frac{1}{q^2-m_\gamma^2}\prod_{i=1}^{4}\frac{1}{(q+p_i)^2-m_i^2},\tag{C.1d}$$

and

$$B_0'\left(p_1,m_\gamma^2,m_1^2\right) = \frac{\partial}{\partial p_1^2}B_0\left(p_1,m_\gamma^2,m_1^2\right),\tag{C.2}$$

which is used in the mm contribution. The integrals are defined in $D=4-2\epsilon$ dimensions in order to regularize the UV divergence in the B_0 function and (if relevant) to regularize possible IR (soft and collinear) singularities in the other functions. The scale μ represents the arbitrary reference scale of dimensional regularization. Sometimes it is convenient to give the arguments of the loop functions in terms of invariants parametrizing the integral, as e.g.

$$B_0\left(p_1,m_\gamma^2,m_1^2\right) \equiv B_0\left(p_1^2,m_\gamma^2,m_1^2\right),\tag{C.3a}$$

$$C_0\left(p_1,p_2,m_\gamma^2,m_1^2,m_2^2\right) \equiv C_0\left(p_1^2,(p_2-p_1)^2,p_2^2,m_\gamma^2,m_1^2,m_2^2\right),\tag{C.3b}$$

$$\begin{aligned}
&D_0\left(p_1,p_2,p_3,m_\gamma^2,m_1^2,m_2^2,m_3^2\right)\\
&\quad\equiv D_0\left(p_1^2,(p_2-p_1)^2,(p_3-p_2)^2,p_3^2,p_2^2,(p_3-p_1)^2,m_\gamma^2,m_1^2,m_2^2,m_3^2\right).
\end{aligned}\tag{C.3c}$$

For the kinematical case considered in Eq. (3.6), i.e. for massless external particles ($m_a, m_b \to 0$ with $m_a, m_b \gg m_\gamma \to 0$), the integrals necessary for Eq. (3.6) are given in the following. The relation '$\sim$' implies that we performed the on-shell projection $\overline{k}_i^2 \to M_i^2$ and set the masses to the real ones, $\overline{M}_i^2 \to M_i^2$, whenever possible. In places where the propagator denominator appears inside a logarithm, $K_i = \overline{k}_i^2 - \overline{M}_i^2$, this is not possible, and K_i is kept with its full dependence on the original momentum $\overline{k}_i^2$. The on-shell projection of the invariants, e.g. $\overline{s}_{ib} \to \hat{\overline{s}}_{ib}$, is implicitly understood to keep the notation brief. The relevant integrals explicitly read

$$\begin{aligned} &D_0\left(m_b^2, \overline{s}_{ib}, \widetilde{s}_{ia}, m_a^2, \overline{k}_i^2, s_{ab}, m_\gamma^2, m_b^2, \overline{M}_i^2, m_a^2\right) \\ &\quad\sim \frac{1}{s_{ab} K_i}\left\{2\ln\left(\frac{m_a m_b}{-s_{ab}}\right)\ln\left(\frac{m_\gamma M_i}{-K_i}\right) - \ln^2\left(\frac{m_b M_i}{M_i^2 - \overline{s}_{ib}}\right) - \ln^2\left(\frac{m_a M_i}{M_i^2 - \widetilde{s}_{ia}}\right)\right. \\ &\qquad\left. - \mathcal{L}\mathrm{i}_2\left(\frac{M_i^2 - \widetilde{s}_{ia}}{M_i^2}, \frac{M_i^2 - \overline{s}_{ib}}{-s_{ab}}\right) - \frac{\pi^2}{3}\right\}, \end{aligned} \tag{C.4a}$$

$$\begin{aligned} &C_0\left(\overline{k}_i^2, \overline{s}_{ib}, m_b^2, 0, \overline{M}_i^2, m_b^2\right) - C_0\left(M_i^2, \overline{s}_{ib}, m_b^2, m_\gamma^2, M_i^2, m_b^2\right) \\ &\quad\sim \frac{1}{\overline{s}_{ib} - M_i^2}\left\{\ln\left(\frac{m_b M_i}{M_i^2 - \overline{s}_{ib}}\right)\left[2\ln\left(\frac{-K_i}{m_\gamma M_i}\right) + \ln\left(\frac{m_b M_i}{M_i^2 - \overline{s}_{ib}}\right)\right] + \frac{\pi^2}{6}\right\}, \end{aligned} \tag{C.4b}$$

$$\begin{aligned} &C_0\left(\overline{k}_i^2, \widetilde{s}_{ia}, m_a^2, 0, \overline{M}_i^2, m_a^2\right) - C_0\left(M_i^2, \widetilde{s}_{ia}, m_a^2, m_\gamma^2, M_i^2, m_a^2\right) \\ &\quad\sim \frac{1}{\widetilde{s}_{ia} - M_i^2}\left\{\ln\left(\frac{m_a M_i}{M_i^2 - \widetilde{s}_{ia}}\right)\left[2\ln\left(\frac{-K_i}{m_\gamma M_i}\right) + \ln\left(\frac{m_a M_i}{M_i^2 - \widetilde{s}_{ia}}\right)\right] + \frac{\pi^2}{6}\right\}, \end{aligned} \tag{C.4c}$$

$$\frac{B_0\left(\overline{k}_i^2, 0, \overline{M}_i^2\right) - B_0\left(\overline{M}_i^2, m_\gamma^2, \overline{M}_i^2\right)}{K_i} - B_0'\left(M_i^2, m_\gamma^2, M_i^2\right) \sim \frac{1}{M_i^2}\left\{\ln\left(\frac{m_\gamma M_i}{-K_i}\right) + 1\right\}, \tag{C.4d}$$

where s_{ab}, $\widetilde{s}_{ia}$, and $\overline{s}_{ib}$ are implicitly understood as $s_{ab}+\mathrm{i}0$, $\widetilde{s}_{ia}+\mathrm{i}0$, and $\overline{s}_{ib}+\mathrm{i}0$, respectively. Here we make use of the function

$$\mathcal{L}\mathrm{i}_2(x_1, x_2) = \mathrm{Li}_2\left(1 - x_1 x_2\right) + \eta(x_1, x_2)\ln\left(1 - x_1 x_2\right), \tag{C.5}$$

which is a specific analytical continuation of the dilogarithm Li_2 in two arguments x_1 and x_2, which in turn makes use of the η function

$$\eta(a, b) = 2\pi\mathrm{i}\Big\{\theta(-\mathrm{Im}a)\,\theta(-\mathrm{Im}b)\,\theta(\mathrm{Im}(ab)) - \theta(\mathrm{Im}a)\,\theta(\mathrm{Im}b)\,\theta(-\mathrm{Im}(ab))\Big\}. \tag{C.6}$$

The remaining C_0 and D_0 integrals can be found in Refs. [43] and [44], respectively. The five-point integral E_0 can be reduced to five four-point integrals D_0 as, e.g., described in Refs. [45, 46].

Finally, we recall the simple, well-known substitution that translates a pure soft IR singularity from mass regularization by the infinitesimal mass m_γ to regularization in $D = 4 - 2\epsilon$ dimensions,

$$\ln(m_\gamma^2) \;\to\; \frac{\Gamma(1+\epsilon)}{\epsilon}(4\pi\mu^2)^\epsilon + \mathcal{O}(\epsilon). \tag{C.7}$$

References

[1] J. Butterworth et al. (2014). arXiv:1405.1067 [hep-ph].

[2] R. G. Stuart. *Phys.Lett.* B262 (1991), pp. 113–119.

[3] A. Aeppli, G. J. van Oldenborgh, and D. Wyler. *Nucl.Phys.* B428 (1994), pp. 126–146. arXiv:hep-ph/9312212 [hep-ph].

[4] A. Denner et al. *Nucl.Phys.* B560 (1999), pp. 33–65. arXiv:hep-ph/9904472 [hep-ph].

[5] A. Denner et al. *Nucl.Phys.* B724 (2005), pp. 247–294. arXiv:hep-ph/0505042 [hep-ph].

[6] P. Gambino and P. A. Grassi. *Phys.Rev.* D62 (2000), p. 076002. arXiv:hep-ph/9907254 [hep-ph].

[7] P. A. Grassi, B. A. Kniehl, and A. Sirlin. *Phys.Rev.* D65 (2002), p. 085001. arXiv:hep-ph/0109228 [hep-ph].

[8] A. Denner and J.-N. Lang (2014). arXiv:1406.6280 [hep-ph].

[9] W. Beenakker, F. A. Berends, and A. Chapovsky. *Nucl.Phys.* B548 (1999), pp. 3–59. arXiv:hep-ph/9811481 [hep-ph].

[10] S. Jadach et al. *Phys.Rev.* D61 (2000), p. 113010. arXiv:hep-ph/9907436 [hep-ph].

[11] A. Denner et al. *Phys.Lett.* B475 (2000), pp. 127–134. arXiv:hep-ph/9912261 [hep-ph].

[12] A. Denner et al. *Nucl.Phys.* B587 (2000), pp. 67–117. arXiv:hep-ph/0006307 [hep-ph].

[13] M. W. Grünewald et al. (2000). arXiv:hep-ph/0005309 [hep-ph].

[14] A. Denner et al. *Phys.Lett.* B612 (2005), pp. 223–232. arXiv:hep-ph/0502063 [hep-ph].

[15] E. Accomando, A. Denner, and A. Kaiser. *Nucl. Phys.* B706 (2005), pp. 325–371. arXiv:hep-ph/0409247 [hep-ph].

[16] M. Billoni et al. *JHEP* 12 (2013), p. 043. arXiv:1310.1564 [hep-ph].

[17] S. Dittmaier and M. Krämer. *Phys.Rev.* D65 (2002), p. 073007. arXiv:hep-ph/0109062 [hep-ph].

[18] S. Dittmaier, A. Huss, and C. Schwinn. *Nucl.Phys.* B885 (2014), pp. 318–372. arXiv:1403.3216 [hep-ph].

[19] A. Denner, R. Feger, and A. Scharf. *JHEP* 04 (2015), p. 008. arXiv:1412.5290 [hep-ph].

[20] V. S. Fadin, V. A. Khoze, and A. D. Martin. *Phys.Rev.* D49 (1994), pp. 2247–2256.

[21] K. Melnikov and O. I. Yakovlev. *Nucl.Phys.* B471 (1996), pp. 90–120. arXiv:hep-ph/9501358 [hep-ph].

[22] W. Beenakker, A. Chapovsky, and F. A. Berends. *Phys.Lett.* B411 (1997), pp. 203–210. arXiv:hep-ph/9706339 [hep-ph].

[23] W. Beenakker, A. Chapovsky, and F. A. Berends. *Nucl.Phys.* B508 (1997), pp. 17–63. arXiv:hep-ph/9707326 [hep-ph].

[24] A. Denner, S. Dittmaier, and M. Roth. *Nucl.Phys.* B519 (1998), pp. 39–84. arXiv:hep-ph/9710521 [hep-ph].

[25] A. Denner, S. Dittmaier, and M. Roth. *Phys.Lett.* B429 (1998), pp. 145–150. arXiv:hep-ph/9803306 [hep-ph].

[26] T. Gleisberg et al. *JHEP* 0902 (2009), p. 007. arXiv:0811.4622 [hep-ph].

[27] S. Höche et al. *JHEP* 1104 (2011), p. 024. arXiv:1008.5399 [hep-ph].

[28] J. Alwall et al. *JHEP* 0709 (2007), p. 028. arXiv:0706.2334 [hep-ph].

[29] R. Frederix, T. Gehrmann, and N. Greiner. *JHEP* 0809 (2008), p. 122. arXiv:0808.2128 [hep-ph].

[30] G. Bevilacqua et al. *Comput.Phys.Commun.* 184 (2013), pp. 986–997. arXiv:1110.1499 [hep-ph].

[31] M. Czakon, C. Papadopoulos, and M. Worek. *JHEP* 0908 (2009), p. 085. arXiv:0905.0883 [hep-ph].

[32] C. Berger et al. *Phys.Rev.* D78 (2008), p. 036003. arXiv:0803.4180 [hep-ph].

[33] G. Cullen et al. *Eur.Phys.J.* C72 (2012), p. 1889. arXiv:1111.2034 [hep-ph].

[34] V. Hirschi et al. *JHEP* 1105 (2011), p. 044. arXiv:1103.0621 [hep-ph].

[35] S. Badger et al. *Comput.Phys.Commun.* 184 (2013), pp. 1981–1998. arXiv:1209.0100 [hep-ph].

[36] F. Cascioli, P. Maierhöfer, and S. Pozzorini. *Phys.Rev.Lett.* 108 (2012), p. 111601. arXiv:1111.5206 [hep-ph].

[37] S. Actis et al. *JHEP* 1304 (2013), p. 037. arXiv:1211.6316 [hep-ph].

[38] A. Denner et al. *Comput.Phys.Commun.* 153 (2003), pp. 462–507. arXiv:hep-ph/0209330 [hep-ph].

[39] M. Beneke et al. *Phys.Rev.Lett.* 93 (2004), p. 011602. arXiv:hep-ph/0312331 [hep-ph].

[40] M. Beneke et al. *Nucl.Phys.* B686 (2004), pp. 205–247. arXiv:hep-ph/0401002 [hep-ph].

[41] A. Bredenstein, S. Dittmaier, and M. Roth. *Eur.Phys.J.* C44 (2005), pp. 27–49. arXiv:hep-ph/0506005 [hep-ph].

[42] B. Jäger and G. Zanderighi. *JHEP* 11 (2011), p. 055. arXiv:1108.0864 [hep-ph].

[43] S. Dittmaier. *Nucl.Phys.* B675 (2003), pp. 447–466. arXiv:hep-ph/0308246 [hep-ph].

[44] A. Denner and S. Dittmaier. *Nucl.Phys.* B844 (2011), pp. 199–242. arXiv:1005.2076 [hep-ph].

[45] D. B. Melrose. *Nuovo Cim.* 40 (1965), pp. 181–213.

[46] A. Denner and S. Dittmaier. *Nucl.Phys.* B658 (2003), pp. 175–202. arXiv:hep-ph/0212259 [hep-ph].